Journal of the European Ceramic Society 38 (2018) 4922–4938

Contents lists available at ScienceDirect

Journal of the European Ceramic Society

journal homepage: www.elsevier.com/locate/jeurceramsoc

Original Article

Life cycle assessment and environmental profile evaluation of lead-free piezoelectrics in comparison with lead zirconate titanate

T. Ibn-Mohammed[a,b,e,*], I.M. Reaney[c], S.C.L. Koh[a,b], A. Acquaye[d], D.C. Sinclair[c], C.A. Randall[e], F.H. Abubakar[a,b], L. Smith[c], G. Schileo[c], L. Ozawa-Meida[f]

[a] Centre for Energy, Environment and Sustainability, The University of Sheffield, Sheffield, S10 1FL, UK
[b] Advanced Resource Efficiency Centre, The University of Sheffield, Sheffield, S10 1FL, UK
[c] Departments of Materials Science and Engineering, The University of Sheffield, Sheffield, S1 3JD, UK
[d] Kent Business School, University of Kent, Canterbury, CT2 7PE, UK
[e] Materials Research Institute, The Pennsylvania State University, University Park, PA, 16802, USA
[f] Institute of Energy and Sustainable Development, De Montfort University, Leicester, LE1 9BH, UK

ARTICLE INFO

Keywords:
Piezoelectric materials
Life cycle assessment
Environmental legislation
Policy and decision making

ABSTRACT

The prohibition of lead in many electronic components and devices due to its toxicity has reinvigorated the race to develop substitutes for lead zirconate titanate (PZT) based mainly on the potassium sodium niobate (KNN) and sodium bismuth titanate (NBT). However, before successful transition from laboratory to market, critical environmental assessment of all aspects of their fabrication and development must be carried out in comparison with PZT. Given the recent findings that KNN is not intrinsically 'greener' than PZT, there is a tendency to see NBT as the solution to achieving environmentally lead-free piezoelectrics competitive with PZT. The lower energy consumed by NBT during synthesis results in a lower overall environmental profile compared to both PZT and KNN. However, bismuth and its oxide are mainly the by-product of lead smelting and comparison between NBT and PZT indicates that the environmental profile of bismuth oxide surpasses that of lead oxide across several key indicators, especially climate change, due to additional processing and refining steps which pose extra challenges in metallurgical recovery. Furthermore, bismuth compares unfavourably with lead due to its higher energy cost of recycling. The fact that roughly 90–95% of bismuth is derived as a by-product of lead smelting also constitutes a major concern for future upscaling. As such, NBT and KNN do not offer absolute competitive edge from an environmental perspective in comparison to PZT. The findings in this work have global practical implications for future Restriction of Hazardous Substances (RoHS) legislation for piezoelectric materials and demonstrate the need for a holistic approach to the development of sustainable functional materials.

1. Introduction

The growing demand for materials and fabrication processes that are environmentally benign, coupled with worldwide policy initiatives and legislations such as the EU directives on Waste Electrical and Electronic Equipment (WEEE) and Restriction of Hazardous Substances (RoHS) [1–8] has encouraged the development of lead-free ceramics for electronic applications. The aforementioned policy initiatives have prompted the replacement of lead and lead components in a number of applications such as solder, paints and a host of other electronic components [9]. Exemptions include technologies and applications based on lead zirconate titanate (PZT) piezoelectric ceramics, where adequate alternatives are not yet available. However, these exemptions are time bound and are discussed and renewed periodically. As such, the veiled threat of removing current exemptions on a permanent basis has triggered important materials development towards lead-free alternatives, considered to be eco-friendly and sometimes purported to have good piezoelectric properties [10].

Piezoelectricity [11] began with the seminal work of the Curie brothers [12] who demonstrated that some crystals do not have a centre of symmetry (e.g. quartz, Rochelle salt, tourmaline and topaz) and possess a reversible property such that the imposition of a dimensional change on the dielectric generates an electrical potential. Conversely, when a suitably oriented electric field is applied, the crystal changes shape (strains) in proportion to the electric field [11]. This reversible

* Corresponding author at: Centre for Energy, Environment and Sustainability, The University of Sheffield, Sheffield, S10 1FL, UK.
E-mail address: t.ibn-mohammed@sheffield.ac.uk (T. Ibn-Mohammed).

https://doi.org/10.1016/j.jeurceramsoc.2018.06.044
Received 3 April 2018; Received in revised form 23 June 2018; Accepted 29 June 2018
Available online 02 July 2018

behaviour is termed the direct and inverse piezoelectric effect, respectively, which are employed in a wide array of sensing and actuating applications [13]. A horde of ground breaking research advances have subsequently been reported, including synthetic polycrystalline ceramics, single crystals and thick/thin films, yielding a tremendous increase in piezoelectric applications [14]. A recent study estimated the global market for piezoelectric actuators alone to be nearly $7 billion, with a steady growth rate of 13% per annum [15]. In addition to the huge market, piezoelectric-based devices also act as drivers for enabling technology in the automobile industry (e.g. fuel atomizers, air flow sensors, audible alarms, and seat belt buzzers), computer sector (e.g. inkjet printers), medical industry (e.g. ultrasonic imaging, foetal heart monitors) and in every day usage such as depth finders, cigarette lighters and telephones.

In recent times, there has been increasing awareness of environmental and health issues related to the presence of > 60 wt% lead oxide (PbO) in PZT-based piezoelectric ceramics [2,16]. The extensive usage of PZT in many products could result in PbO being released into the atmosphere during its life cycle. The emission of PbO from PZT-based products could take many forms, such as evaporation from the starting oxides during calcination and sintering and leakage through machining or improper waste disposal. Accordingly, the need to minimise effects of toxic PbO release into the environment whilst safeguarding human health, forms the basis of the WEEE and RoHS legislations pertaining to PZT. Aside from drawbacks based on environmental considerations, the presence of lead also confers a density that is relatively high, a property that constitute a huge hindrance in some applications due to high acoustic impedance [11]. These issues coupled with the threat of removing exemptions have promoted the development of lead-free piezoelectric materials, based around Nb_2O_5 and Bi_2O_3 containing complex oxides [16–23], which have yielded encouraging progress, since the landmark findings by Saito et al. [5]. Further recent advances are described in detail in [15,24].

Given the findings by Ibn-Mohammed et al. [10,25] that KNN is not intrinsically ‘greener’ than PZT, there is a tendency to see NBT and its potassium analogue, KBT, as the solution to achieving an environmentally green lead-free piezoelectric materials [16,23]. NBT and KBT are both endowed with moderately high Curie temperatures of 593 and 653 K, respectively [26] and NBT-based solid solutions exhibit large strains (0.4%) [9]. However, the high coercive field of NBT-based composition (73 kV/cm), their high conductivity, low depolarisation temperature [27], large hysteresis and difficult control of stoichiometry due to volatilisation during sintering [27] are problematic [28]. Various dopants [28–35] have thus been employed to mitigate these issues whilst enhancing properties [27].

Before a successful transition from laboratory to market, a critical environmental assessment of all aspects of the fabrication and development of NBT lead-free piezoelectric materials must be carried out in comparison with PZT. Concerns about the “health” of our planet necessitate a careful evaluation of the environmental profile of the proposed lead-free materials in comparison to the lead-based materials before any valid claims of the environmental edge of one material over the other can be made and before expensive investments and resources are committed towards upscaling. Against this backdrop, the current work adopts a quantitative framework of hybrid life cycle assessment (HLCA) and presents comprehensive cradle-to-grave environmental impacts of lead-free NBT within a holistic process design framework. LCA is a computational technique which evaluates the complete environmental impact of a material or product, including the raw materials extraction, materials processing, application, and disposal [36].

We live in a world interconnected by networked product supply chains, multifaceted production technologies, and consumption patterns that are nonlinear [8,37]. As such, finding ways to align sustainable supply chain strategies to the challenges of piezoelectrics is important if the boundaries of materials substitution and their associated environmental impacts are to be pushed. LCA can be used to track material flows in production processes through a materials development strategies and by identifying priorities for improvement with policy makers and environmental regulators. For materials substitution to be adjudged viable, it must offer either technical advantages over its traditional counterpart, and/or an excellent environmental and social footprint [10]. Consequently, the research questions addressed in this paper are:

- Where do the environmental and carbon hotspots of NBT functional ceramics lie across multiple environmental indicators and how does the environmental profile of NBT compare to the traditional PZT functional ceramics, given that bismuth from is derived as a by-product of lead smelting?
- How does the environmental profile of NBT compare to KNN? The environmental profile of lead-free piezoelectric ceramic such as KNN has been identified to be worse compared to PZT due to the presence of ~60 wt.% Nb_2O_5, whose mining and extraction cause significant environmental damage [10,25].

To answer these questions, the overall environmental profile of NBT is analysed across multiple environmental indicators. The results are then compared with the environmental profile of PZT and KNN based on results already published by Ibn-Mohammed et al. [10,25]. Details of the overall methodological framework of the LCA model and the data sources for constructing the life cycle inventory is provided in Section 2. In Section 3, key findings are analysed and discussed, highlighting the implications for piezoelectric material development, followed by conclusions in Section 4.

2. Research methodology

The LCA in this work is based on the following standard four key steps: (i) definition of goal and scope, where questions such as what, how and why pertaining to the LCA work are examined and where the systems boundaries and functional unit are established; (ii) analysis of the inventory in which inputs and outputs data of each process in the life cycle as well as data related to impact categories are systematically collected and integrated across the entire system; (iii) evaluation of the environmental effects, detailing LCA calculations and results through classification and characterization for comparative analysis; (iv) the interpretation of the inventory and impact assessment of results, from where environmental hotspots are identified [36,38,39].

All inventories are appropriately converted to conform to the 1 kg functional unit based on the defined systems boundary, as illustrated in Fig. 1. The overall focus of the current work is on global warming potential (GWP). However, the need to consider multiple environmental indicators when analysing the environmental profile of a product or process has been demonstrated by a number of authors including Hoekstra and Wiedmann [40]; Ibn-Mohammed et al. [25]; Azapagic et al. [41] and Zhang et al. [42]. This allows environmental trade-off analysis, whilst ensuring that greenhouse gas (GHG) emissions are not abated at the expense of other environmental indicators [43]. Accordingly, to account for the individual contributions of process exchange

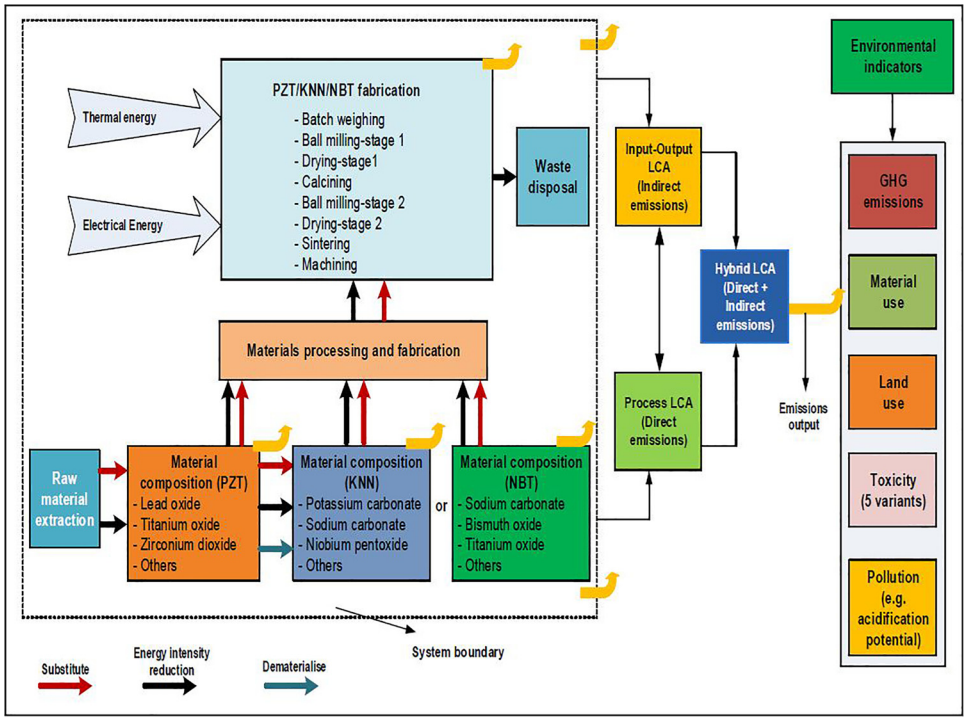

Fig. 1. System boundary for LCA, detailing relevant material and energy flows recorded in the inventory. Only main constituent materials and environmental indicators are shown for brevity. Five variants of ecotoxicity: marine aquatic; marine sediment; fresh water sediment; fresh water aquatic and terrestrial and human toxicity are also considered alongside malodours air and ionisation radiation. Functional unit of "per kg material produced at the laboratory scale" is adopted. For other input resources, see Electronic Supplementary information (ESI).

entries into the lifecycle system, the LCA in this work is conducted, from cradle-to-grave, across multiple environmental indicators, based on Centrum voor Milieuwetenschappen Leiden (CML) impact assessment method [44] including climate change (i.e. GHG emissions), land use, acidification and eutrophication potentials as well as cumulative energy demand. Five variants of ecotoxicity: marine aquatic; marine sediment; fresh water sediment; fresh water aquatic and terrestrial and human toxicity are also considered alongside malodours air and ionisation radiation. Three endpoint indicators (ecosystem quality, human health and resources) based on Eco indicator 99 methodology [44] are also taken into account.

In this work, the quantitative framework of HLCA [25,38,45–48] integrates the process-based [41,49] LCA inventories with Environmental Input-Output (EIO) [50–52] data to compute the environmental burden of a laboratory-based NBT piezoelectric material.

2.1. Process-based LCA modelling

The overall impact assessment based on the LCI was performed in accordance to the guidelines provided in the International Organization for Standardization (ISO) 14040 [53] and 14044 [54]. Each entry within the LCI developed for this work was matched with an appropriate unit process in conformity with the defined functional unit. Based on the process LCA, the environmental impacts were calculated as follows [25,41,49]:

$$Process\ LCA = \sum_{i=1}^{n} A_{p(i)} \times E_{P(i)} \quad (1)$$

where: A_p is the inputs (i) into a product's (i.e. NBT piezoelectric materials) supply chain including raw material extraction, energy consumption during fabrication processes, and material production, etc.; n is the total number of process input (i) into the NBT's supply chain and E_P is the emissions intensity across a number of environmental indicators, for each input (i) into the emissions associated with the supply chain of NBT. All data used within the process-based LCA framework are based on the NBT production route as described in the subsection that follows.

2.1.1. Production route for NBT

In this section, procedures for fabricating NBT are presented. For comparison with KNN and PZT, laboratory-based temperatures and sintering times for undoped NBT are employed, although we note production routes vary with manufacturer. This is particularly true when dopants and substituents are used to modify and improve the piezoelectric properties.

The fabrication route for NBT-based compositions (Fig. 2) is similar to that of PZT and KNN with the starting materials: sodium carbonate (Na_2CO_3); bismuth oxide (Bi_2O_3) and titanium oxide (TiO_2). The correct stoichiometric quantities are calculated for the desired composition before the mixture is ball-milled in iso-propanol for 6 h to ensure that all powders are mixed thoroughly together. This allows for the homogenous mixing of the powder and reduction in particle size, whilst ensuring a complete solid state reaction. The resulting slurry is dried at ~80 °C overnight, sieved and calcined at 800 °C for 2 h. The resultant powder is subjected to a final round of ball milling for 6 h, dried, sieved and pressed into pellets by uni-axial pressing followed by isostatical pressing at 200 MPa. Pellets are embedded in sacrificial powder of the same composition and sintered at 1150 °C for 2 h in air.

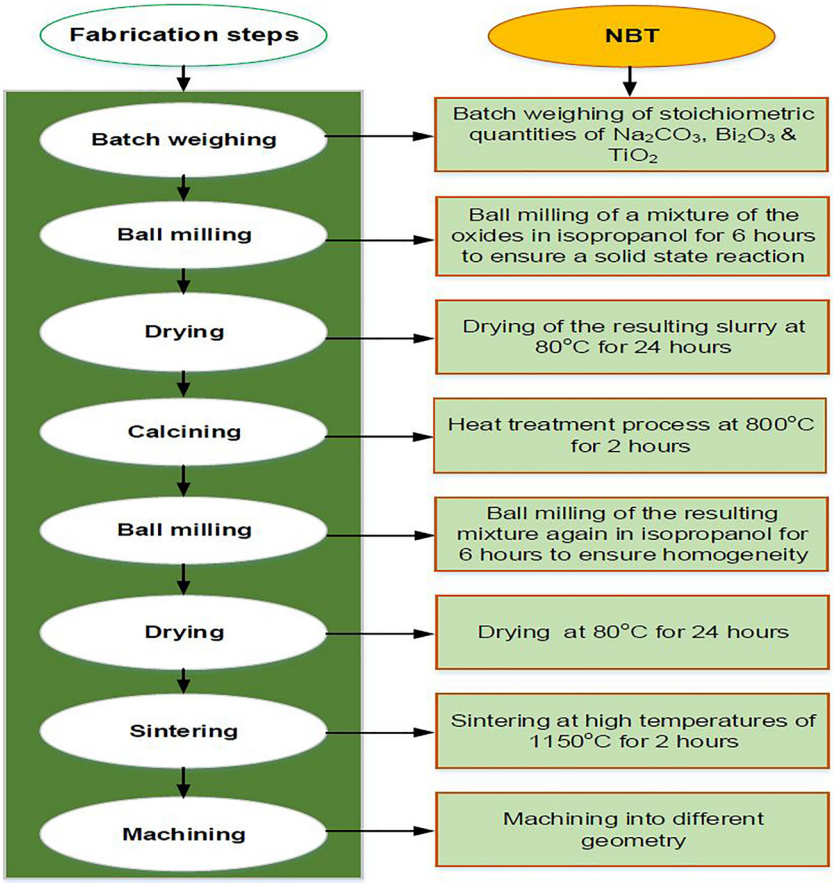

Fig. 2. Fabrication route of NBT piezoelectric material. Typical laboratory-based times and temperatures are quoted for comparison but it is anticipated that these may be modified slightly for commercial production for different manufacturers. The fabrication steps described an in line with those in extant literature on the synthesis of NBT. See Lencka et al. [26] and Chou et al. [28].

2.1.2. Process-based LCA data source

Data requirements for the LCA is informed by key steps namely: i) gaining an understanding of the NBT piezoelectric material based on raw material requirements, production and fabrication procedures; ii) characterisation of the system boundary and setting of an appropriate functional unit; iii) construction of the LCI based on input requirements (i.e. physical processes), supply chain and embodied emissions data, process flow, energy flow, material and flow; iv) overall impact assessment and environmental profile evaluations across multiple sustainability metrics and v) performance evaluation and analysis.

Process data for inputs into the LCI are based on inventory data estimated from laboratory processes (Fig. 2) such as engineering heuristics and study assumptions, Ecoinvent database [44] and well-established data from within the literature. Process data input into the LCA system boundary (Fig. 1) includes emissions arising from raw material extractions, fabrication processes in terms of electrical and thermal energy consumption regarding NBT production. Given that all fabrication operations are carried out using electrical equipment in the laboratory, the electrical energy consumption (kWh) is calculated by multiplying the electrical power (W) of the specified device as described by the manufacturer by the time (sec) during which the specific temperature is maintained for each of the processes. To account for heating demand for the fabrication processes, where temperature is increased from an ambient to a desired temperature, the required energy (Q) is calculated by multiplying the specific heat capacity of the material heated (J/kg·K), mass of material heated in the process (kg) and temperature difference (K or °C). See ESI for electrical and thermal energy consumption data for the fabrication of NBT.

All emissions intensity data across all the indicators were taken from Ecoinvent database [44]. For certain materials, whose emissions intensity are not available, such data were derived on the basis of stoichiometric reactions from previously published guidelines [55] or direct substitution from chemical characteristics or functional similarities. In particular, emissions intensity data for bismuth (a key material in the development of NBT) which is not available in Ecoinvent database, a newly developed dataset based on the framework described briefly in Section 2.1.3 was adopted to derive such data across multiple environmental indicators. All data sources of the unit process exchanges (i.e. individual material entries) representing the process analysis data are presented in the ESI.

2.1.3. Derivation of emissions intensity data for bismuth oxide

The emissions intensity data for bismuth and its compounds are not available in Ecoinvent and other related LCA databases. It is therefore, difficult to derive its emissions intensity data on the basis its elemental form. As such, it is important to gain an understanding of the extraction/production processes of bismuth. This will put into perspective the environmental lifecycle of bismuth and its oxides for NBT.

In the Middle Ages bismuth was recognised but often confused with lead, tin, zinc and antimony, given the difficulty in isolating the metal [56]. However, research by Johan Heinrich Pott and Claude Geoffrey in the mid-18th century provided insight into its unique properties. An important discovery was the awareness by medical practitioners regarding some of the beneficial properties of bismuth for the treatment of gastric conditions. Over the years, the lead-free agenda has adopted bismuth in many applications.

Bismuth is commonly found naturally in the sulphide ore known as bismuthinite (Bi_2S_3) and is regarded as the most important bismuth mineral. Bismuth is rarely found in nature in its elemental form and its extraction solely for bismuth content is rarely economical. As such, bismuth is primarily obtained as a by-product of lead and copper smelting and sometimes from tin, tungsten and zinc ores from China. The primary process for the recovery of bismuth differs depending on the minerals and the major metal mined. However, the refining

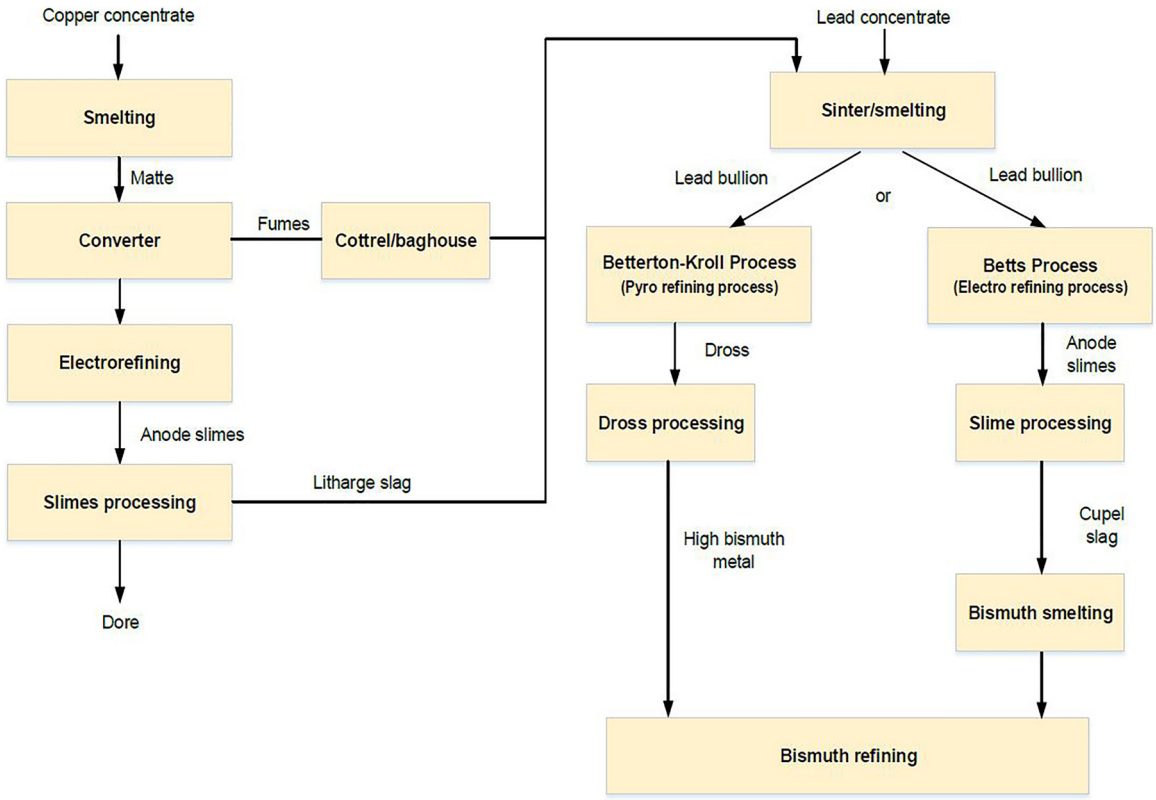

Fig. 3. The transfer of bismuth in process residues from copper to lead smelting and subsequent recovery. Reproduced from Ref. [56].

processes are invariably identical. Very small portions (roughly 0.5%) of current world production is available from mines worked specifically for bismuth. In China and Bolivia, for example, bismuth concentrate (typically oxide or carbonate) is leached with hydrochloric acid. Bismuth is precipitated as bismuth oxychloride after repeated dissolution and precipitation removes several soluble impurities. The dried oxychloride is smelted with carbon using soda ash flux to produce crude bismuth bullion.

The primary extractive process for most market-available bismuth occurs via one of two processes: (i) the *Betterton-Kroll Process* (i.e. the pyro refining process for lead) and (ii) the *Betts Process* (i.e. the electro refining process for lead) [57]. The choice of one process over the other depends on the strategy for lead refining rather than bismuth production. Each process is adopted by different companies in different countries [58]. The Betterton-Kroll Process isolates bismuth from lead by introducing calcium or magnesium into a molten solution of lead and bismuth. The resulting calcium or magnesium bismuthide which is less heavy than molten lead rises to the surface as dross (solid impurities) which can then be removed. The dross is then subjected to treatment with chlorine at temperatures between 380–500 °C to remove the magnesium or calcium [57,58]. High purity bismuth is produced after treatment using sodium hydroxide.

On the other hand, the Betts Process encompasses electrolytic refining of lead bullion. It is based on the dissolution of a lead anode in a fluorosilicic acid and its deposition on a cathode, while impurities, including bismuth, settle to the bottom of the vessel. The muddy mix of metals can be melted to produce metal alloy and bismuth-rich slag, which is then reduced with carbon to produce bismuth metal [57,58]. Fig. 3 provides a pictorial representation of the transfer of bismuth in process residues from copper to lead smelting and subsequent recovery based on the two processes. For detailed description of both processes, see Terrado [58].

In the description of the above production and recovery processes, the quantity of bismuth obtained represents a small fraction by mass (typically < 1%) in comparison to other co-products [59–62]. However, bismuth is a moderately priced metal, costing more than copper, lead, and zinc, but less than gold or silver. Substitution and systems expansion are therefore not feasible given the impossibility of identifying neither an alternative production process for bismuth nor potential substitute. Additionally, allocation by mass partitioning yields almost zero impacts on bismuth. There is no way to avoid allocation by identifying a routine which only yields bismuth given that all the involved co-products are derived from the same input. As such, economic allocation [63,64] on the basis of parameters such as price or revenue, is a better approach given that it reflects the causality of the production and recovery process. This is in line with the stepwise approach detailed in ISO 14044 which recommends that economic allocation is applied as a last resort when other alternatives are not feasible or suitable. Nevertheless, the scientific debate on the applicability of economic allocation is unending given the different and sometimes contrasting opinions among LCA practitioners. Ardente and Cellura [64] provided a state of the art discussion on economic allocation in LCA across a number of sectors including food, construction and biofuels.

In a shared process providing co-products or co-services, the economic partitioning or allocation factors are calculated as the share of the proceeds of one product or service in the total outcome of the proceeds of all products based on the relation [64]:

$$P_i = \frac{n_i . x_i}{\sum_i n_i . x_i} \quad (2)$$

where p_i is the partitioning factor of the ith co-products or co-services, n_i is the quantity of the ith product/service, x_i is the price of the ith co-products or co-services and $n_i . x_i$ is the magnitude of the functional flow i as it enters process 1, measured based on financial revenue

To derive the data for the environmental profile of bismuth based on the above methods, we expand upon the work of Andrae et al. [61] and

Nuss and Eckelman [60], using their inventory data and uncertainty ranges for each parameter. The original data set by Andrae et al. [61] was mostly based on Canadian company sustainability reports which are publicly available, where bismuth is derived as a by-product from lead-zinc mining and refining. For the economic parameters adopted in the calculation procedures, market prices and by extension allocation percentages adopted by Andrae et al. [61] were updated to reflect the current average price of bismuth based on USGS data. For full details of the emissions intensity data of bismuth and by extension bismuth oxide, we refer readers to the ESI.

2.2. Rationale for using hybrid LCA

As with all LCA studies, getting access to all data inputs necessary to conduct analysis at a determined level of detail based on all the areas identified in the goal and scope definition stage of the study can be very challenging to obtain and time consuming. For example, in this work, data including contributions from upstream processes such as the use of imported equipment, special purpose machinery, transportation, telecommunications, research and development as well as other related business services, which forms part of the overall development of piezoelectric materials are not available. It is important not to ignore the impact of the contributions from such activities. An estimation of such contributions using a well-established framework such as hybrid LCA is far better than an explanation regarding the lack of data or even ignoring the effects altogether [25]. Although authors such as Zamagni et al. [65] suggest caution with the use of hybrid LCA, nevertheless, the current work augments process-based LCA with EIO LCA to ensure completeness of the analysis whilst taking into account the missing inputs from process-based LCA. There are different variants of HLCA and how each is setup provides added value based on the system under consideration. A brief description of EIO LCA is presented in the section that follows.

2.3. Environmental input output LCA modelling

The general IO model is a quantitative technique employed to interprete the flows of goods and services within a specific economy [66] whilst allowing the examination of the interrelationships between each economic sector over a given time frame [67]. The basis of IO analysis is the IO table which shows the flow of goods and services from one industry to other industries (rows) and the inputs required by an industry to produce its outputs (columns). The EIO LCA is carried out by linking national IO tables with direct industrial emissions intensities to compute the upstream indirect emissions associated with the inputs into the supply chain for the production of the final product [67,68]. The technique entails the conversion of economic flows into physical flows using well-established assumptions of IO analysis. In doing so, the relationship between economic activities and environmental impacts attributed to downstream activities can be established [46,69]. Detailed explanation of the IO framework is well documented in literature [70–72]. Let$A_{i,o}$ represent the technical coefficient IO matrix, (I) the identity matrix, $E_{i\,o}$ the direct emissions intensities across a number of sustainability metrics for each IO industry and (y) the final demand [70], the EIO model can therefore be expressed as:

$$EIO\ LCA = E_{i\,o}\cdot(I - A)^{-1}\cdot y \tag{3}$$

where: $E_{i\,o}\cdot(I - A)^{-1}$ is the total (direct and indirect) emissions intensities of each industry required to produce a unit of product. The use of EIO allows for the evaluation of latent, or upstream or indirect (these adjectives are often adopted interchangeably) embodied environmental impacts related to a downstream consumption activity, such as the total emissions that occur when a product is bought and consumed [69].

2.3.1. Input-output data

In this work, Supply and Use (S&U) input-output tables for the UK and the rest of the world (RoW) represented as (896 × 896) technology matrix to compute upstream indirect emissions in the LCA framework was adopted. Additionally, data for all environmental indicators are obtained representing the sectorial environmental intensities (i.e. kg CO_2-eq/£ for GHG, kg SO_2-eq/£ for acidification potential, kg NO_x-eq /£, for eutrophication potential, kg/£ for toxicity, m^2a/£ for land use and MJ/£ for material usage for the environmental matrix, $E_{i\text{-}o}$), from World Input-Output Database (WIOD) [73] and expanded upon to conform to the 896 × 896 MRIO framework. Refer to Supplementary Fig. S2 in the ESI. The WIOD consist of national IO tables, MRIO tables, environmental accounts for forty countries and one RoW category comprising all other regions. The IO table in each country consist of 56 × 56 economic sectors. Given that the technology matrix $A_{i\,o}$ in this study is a (896 × 896) MRIO technology matrix and describes input and output coefficients requirements from one sector to another within the UK vs. RoW S&U MRIO framework, it is important to make the IO environmental intensities of other indicators conform with the same framework. As such, 39 countries (i.e. excluding the UK) and one RoW were aggregated to become an “integrated” RoW. For details on how the IO data datasets were derived, see ESI.

2.4. Multi-Regional Input-Output (MRIO) hybrid LCA model

By integrating both Eqs. (1) and (3) using matrices algebra [74], a hybrid LCA model, as shown in Eq. (4), is established, allowing for both upstream and downstream linkages between the two LCA systems to be evaluated. The consistent mathematical framework incorporating the environmental indicators of GHG, material use, land use, acidification, eutrophication, and toxicity for the hybrid LCA within a Multi-Regional Input-Output (MRIO) framework, is defined as follows:

$$Hybrid\ LCA = \begin{bmatrix} E_{p(g,m,i,p,t)} & 0 \\ 0 & E_{io(g,m,i,p,t)} \end{bmatrix} \begin{bmatrix} A_p & -C_d \\ -C_u & I - A_{i\,o} \end{bmatrix}^{-1} \begin{bmatrix} y \\ 0 \end{bmatrix} \tag{4}$$

&thisp;$E_{p(g,m,i,p,t)}$ Process inventory environmental extension matrix for GHG, material and land use, pollution (e.g. acidification and eutrophication potentials), and toxicity. All metrics are measured in their respective units (e.g. kgCO_2-eq for climate change) and diagonalised, (dimension:m× s)

$E_{i\,o(g,m,i,p,t)}$ MRIO environmental extension matrix for GHG, material use, land use, water use, pollution and toxicity. All metrics are measured in their respective units (e.g. kgCO_2-eq per £ for GHG) and diagonalised (dimension: m× s)

A_p Square matrix representation of the process LCA inventory, (dimension: s× s)

$A_{i\,o}$ Input- Output technology coefficient matrix, (dimension: m× m)

I Identity matrix, (dimension: m× m)

c_u Matrix representation of upstream cut-offs to the process system, (dimension: m× s)

c_d Matrix of downstream cut-offs to the process system, (dimension: s× m)

$\begin{bmatrix} y \\ 0 \end{bmatrix}$ Functional unit column matrix with dimension: $(s + m, 1)$, where all entries are 0 except y

Hybrid LCA (i.e. total impacts) is the direct and indirect environmental impact associated with one unit of final demand y for the product (here NBT). Matrix A_p describes the product inputs into processes as captured in the unit process exchanges (i.e. process LCA system). A_{i-o} in this study is a (896 × 896) multi regional input-output (MRIO) technology matrix and describes input and output coefficients requirements from one sector to another within the UK vs. RoW Supply and Use MRIO framework. Matrix U which is assigned a negative sign,

Table 1
Hybrid LCA results for NBT material system.

Impact category	Process	EIO	Hybrid (Total)
Climate Change (kg CO_2-eq)	30.374	6.153	36.53
Acidification potential (kg SO_x-eq)	0.135	0.004	0.14
Eutrophication potential (kg NO_x-eq)	0.079	0.008	0.09
Land use (m^2a)	0.789	0.588	1.38
Material use (MJ-eq/kg)	447.026	42.530	489.56

represents the higher upstream inputs from the MRIO system to the process system. Matrix D, also assigned a negative sign, represents the (downstream) use of goods/process inputs from the process to the background economy (MRIO system). The negative signs represent the direction of flow of inputs. For further details on how the overall multi-metric hybrid LCA framework is developed, see Ibn-Mohammed et al. [25].

Due to data availability issues [75] and for the purpose of simplicity [76], MRIO frameworks are usually presented as a 2-region model. Such two-regional models have been applied in a wide range of studies [51,77,78]. In the context of this work, a 2-region MRIO model interlinking the UK and the RoW was adopted. This is because the aggregation of the other entire world countries into a single region is a limitation as there are technology differences between different countries [51]. Additionally, in instances where the UK is an importer, distinct supply chains between country of production and the UK cannot be established. The approach therefore takes a system-wide view of embodied energy analysis and allows for multi-regional analysis of embodied emissions associated with products. More importantly, adopting a 2-region model allows for ease of implementation within the overall hybrid LCA framework. As efforts are been made to build a global MRIO model with distinct country specific data [79], this research can be extended in the future to overcome the data issue and limitations.

3. Results, analysis and discussion

3.1. Life cycle impacts of NBT fabrication

3.1.1. Hybrid life cycle assessment of laboratory-based NBT ceramics

The overall environmental profile of the NBT material system is estimated as the integration of the process-based and the EIO-based LCA across the five environmental indicators of interest. The IO indirect upstream emissions comprise embodied emissions attributed to, amongst others, equipment, chemicals, maintenance, research and development, banking and finance, transportation, telecommunications, insurance and advertising not accounted for in the process LCA system. How process-based results compare to EIO results is shown in Table 1 and represented in graphical form in Fig. 4.

An examination of the toxicology environmental impacts (Fig. 5) along the production routes of NBT ceramic indicates that marine sediment ecotoxicity has the highest toxicology impact. Due to the numerous number of chemicals included in the input-output inventory of toxic release database, it was difficult to express upstream toxic impacts in kg 1, 4-DCB-eq.

In the subsections that follow, component level analysis based on process-based LCA as well as sectoral level analysis by EIO LCA of the environmental impacts of NBT fabrication is presented to identify the most influential components and materials as well as economic sectors. For instance, as shown in Fig. 4, based on climate change environmental indicator, the total impact is 37 kg CO_2-eq (31 kg CO_2-eq and 6 kg CO_2-eq for process and EIO LCA calculations, respectively). The aim of the next sections is therefore to identify the proportion of each material or process within the life cycle inventory that contributes to ~31 kg CO_2-eq and the economic sector that contributes to the ~6 kg CO_2-eq from the EIO LCA. This allows the identification of environmental hotspots and the corresponding materials/process responsible for such hotspots for which mitigation may be recommended. Given that primary energy consumption is an integral part of the overall environmental profile of NBT, a detailed breakdown is provided in Section 3.1.2.

3.1.2. Primary energy consumption for fabrication of laboratory-based NBT ceramic

Primary energy consumption (both electrical and thermal) and material embedded (i.e. cumulative energy demand) for the fabrication of the NBT ceramic are shown in Fig. 6, totalling 447.02 MJ-eq/kg. As indicated in Fig. 6(a), the primary energy consumed in fabrication contributed to about 75.88% (339.18 MJ-eq/kg); that is 75.8% electrical energy and 0.08% thermal energy of the total primary energy consumption. High electrical energy is required in the fabrication stage of NBT due to the length of time required to complete the drying, calcining and sintering operations. A breakdown of the thermal energy consumed (Fig. 6(b)) during manufacturing indicate that relatively long

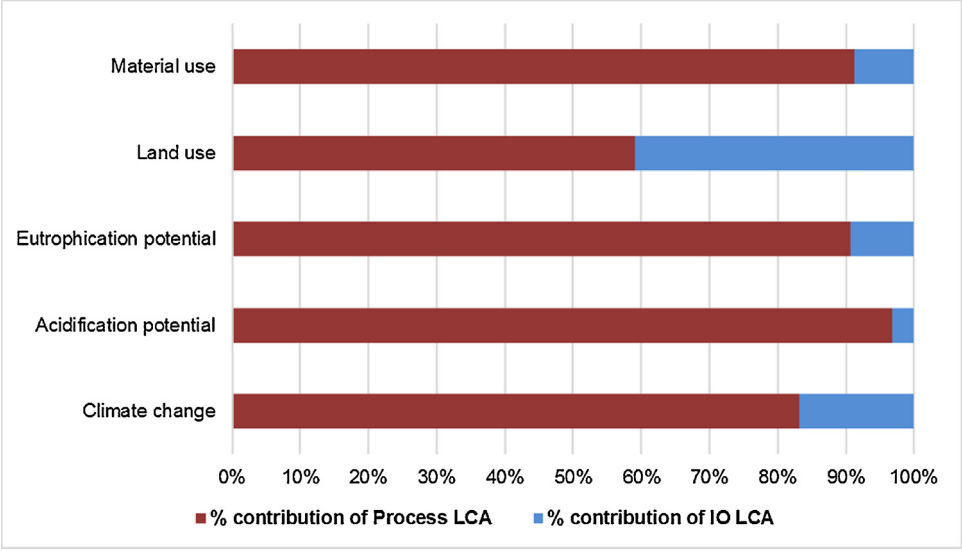

Fig. 4. Results of hybrid LCA (process + IO) of NBT across five environmental indicators are based on a functional unit of 1 kg material produced at the laboratory scale.

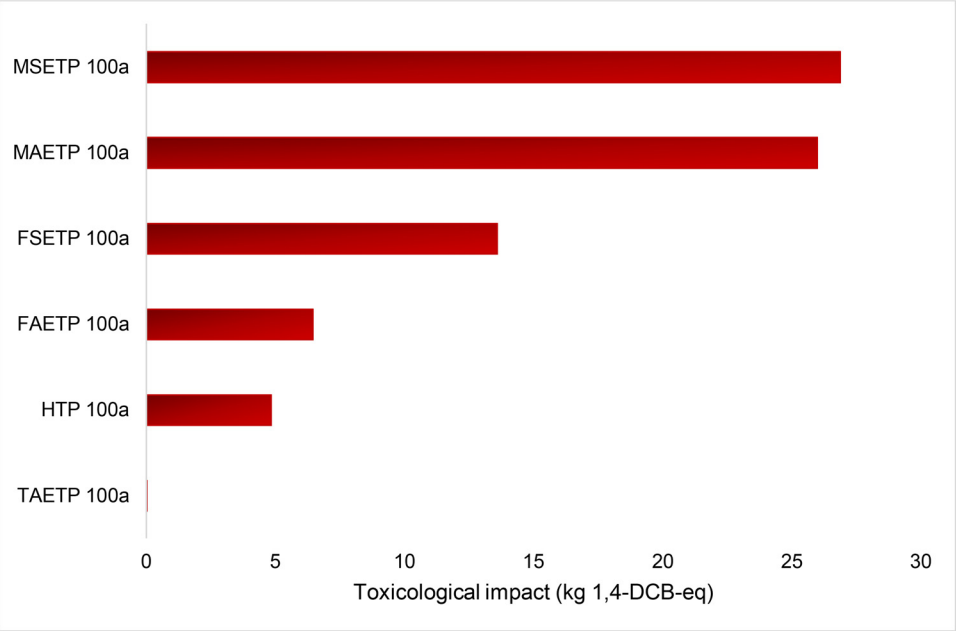

Fig. 5. Toxicological impact of NBT across six variants of toxicity.

duration and high temperature sintering results in the highest thermal energy demand (44%) with calcination and drying responsible for 34% and 22%, respectively.

The percentage contributions of each of the process steps regarding electrical energy consumption is shown in Fig. 6c, with ball milling responsible for 69% of the total electrical energy demand. Raw material requirements constitute the remaining 24.1% (107.84 MJ-eq/kg). A breakdown of the materials embedded in NBT manufacturing (Fig. 6(d)) shows that bismuth oxide is the most influential component, contributing 69% of the material impact category. Titanium oxide and sodium carbonate are responsible for 29% and 2% respectively of materials embedded in NBT ceramics fabrication. As commented by Ibn-Mohammed et al. [25] optimised sintering approaches such as the use of sintering aids and low temperature processing technology (e.g. cold sintering [80–82]) can contribute to the overall reduction in thermal and electrical energy demand for fabrication of functional materials.

3.1.3. Analysis of the environmental profile of NBT ceramics based on the contributing processes

Fig. 7 shows the environmental profile of all the unit process exchanges representing the analysis data of 1 kg of NBT ceramic fabricated in the lab. All the 13 environmental indicators are normalised, ensuring that the absolute indicator of each category of impact is 100%. As indicated in Fig. 7, most of the environmental impact emanates from high amount of electricity utilised during the fabrication of NBT ceramic, except in malodours air impact category where the influence of titanium dioxide dominates by 56%. However, in terms of the actual materials constituents, bismuth oxide and titanium dioxide also dominate across the listed environmental indicators. For instance, the use of bismuth oxide is the second largest contributor to climate change (40%), acidification (38%), eutrophication (39%), land use (41%), material use (17%), fresh water aquatic ecotoxicity (39%), fresh water sediment ecotoxicity (39%), human toxicity (38%), marine aquatic ecotoxicity (39%), marine sediment ecotoxicity (39%), terrestrial ecotoxicity (39%), ionising radiation (42%) and malodours air (18%).

The environmental burden of bismuth and its oxide are mainly due to the purification (i.e., smelting) and refining stages required to obtain the final metal product. Bismuth compounds (e.g. Bi_2O_3) account for roughly half the production of bismuth. Bi_2O_3 is generally considered the most important compound of bismuth given its vast industrial application and it is the common starting point for the chemistry of bismuth metal. The high climate change impact of Bi_2O_3 pertains to the high amount of energy required during its purification and refining given that it is usually obtained as a by-product of smelting of copper and lead [57,60,83]. In particular, the purification procedures contribute more to the overall impact because intermediate products such as anode slime and leaching residue are included in the overall assessment.

In this work, the starting material for the derivation of emissions intensity for Bi_2O_3 across multiple environmental indicators was Bi_2S_3. The preparation of Bi_2S_3 was based on the direct reaction of elemental bismuth with elemental sulphur in an evacuated silica tube at 500 °C for 4 days. Bi_2O_3 is then obtained by roasting the sulphide ore (i.e. Bi_2S_3). In the instance where the final targeted product is bismuth, Bi_2O_3 is reduced with carbon to form bismuth. For details of how the emissions intensity of Bi_2O_3 is derived, see ESI. The reported values across the six variants of toxicological impact pertain to leaching of bismuth concentrates such as its oxide with hydrochloric acid from which bismuth is precipitated as bismuth oxychloride after repeated dissolution, from which several soluble impurities are removed by precipitation. Although the percentage contribution of the toxicity impacts due to processing and purification of Bi_2O_3 within the NBT materials systems is relatively high (second after impact from electricity utilisation), the toxicity of bismuth is considered low since bismuth compounds are poorly absorbed [62]. Its lower comparative toxicity is the underlying reason that it is gaining a great deal of momentum as a substitute for lead in manufacturing processes where RoHS compliance criteria are gaining importance.

As such, neither the World Health Organisation (WHO) regarding guidelines for drinking water nor the U.S. Department of Labour Occupational Safety and Health Administration (OSHA) concerning permissible exposure limits (PEL), have reported any limit values for bismuth as part of alloys except OSHA 10 mg/m^3 for dust emanating from undoped bismuth telluride [61]. Accordingly, bismuth and its oxides are not a key target materials of RoHS compliance (compared to lead within a range of non-exempt manufacturing processes). However, in recent times, bismuth has been classified as toxic and its compound have been included in the materials declaration of a number of Silicon Valley semiconductors manufacturers [84]. For instance, IT giant such as Hewlett-Packard (HP) has included bismuth in their list of substances

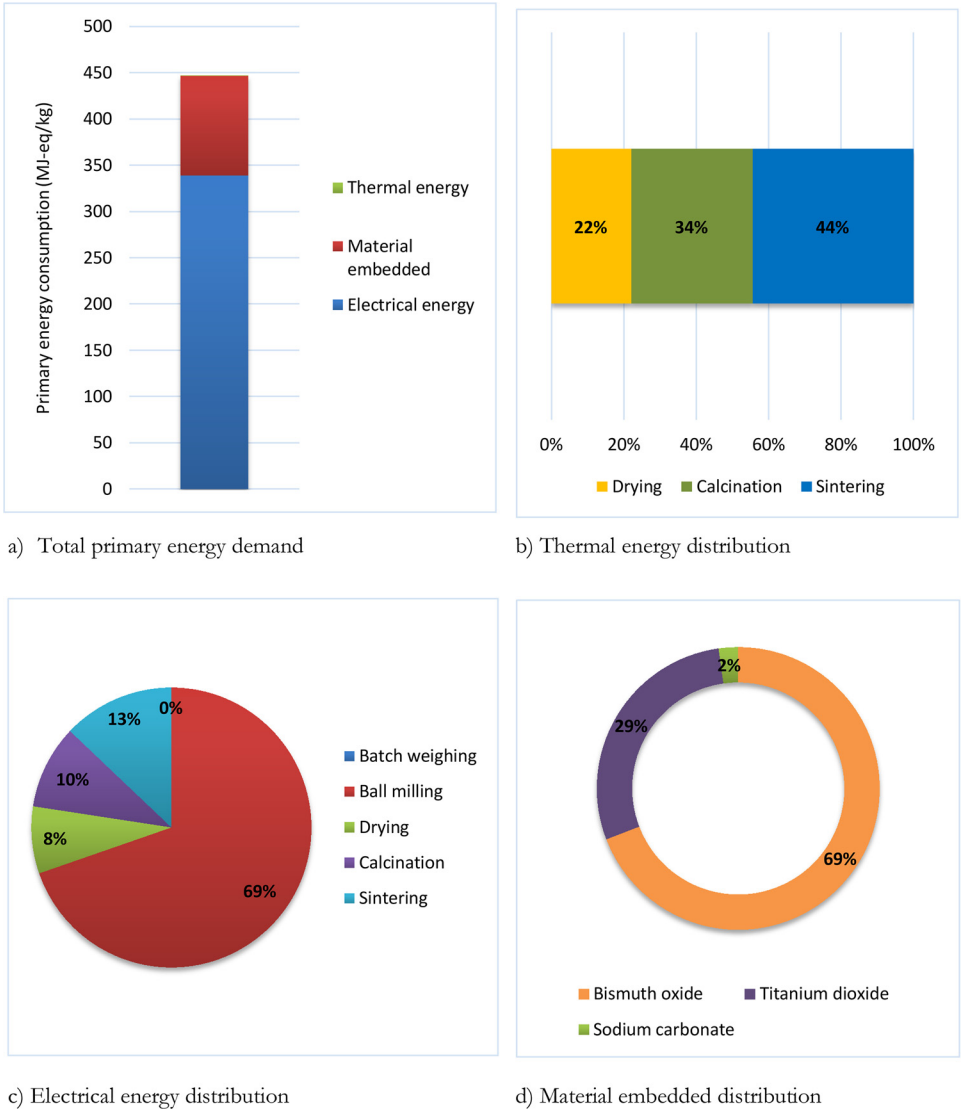

a) Total primary energy demand

b) Thermal energy distribution

c) Electrical energy distribution

d) Material embedded distribution

Fig. 6. Distribution of the primary energy consumption for the fabrication of a laboratory-based NBT piezoelectric material: (a) total primary energy consumption including thermal and electrical energy and materials embedded all expressed in MJ-eq kg^{-1}; (b–d) indicate the percentage contributions of each process or material relative to (a).

for further evaluation “for possible future elimination or restriction”, alongside more familiar compounds including beryllium, mercury and arsenic [84].

Given that lead is the most immediate economic and environmental comparator to bismuth, it is important to look into the details of the environmental impacts of Bi_2O_3 and PbO within the NBT and PZT and by extension compare the overall environmental profile of lead and bismuth. As shown in Fig. 8, it is interesting to note that under climate change environmental indicator, the impact of NBT (30.4 $kgCO_2$-eq), for example, is lower than that of PZT (44.4 $kgCO_2$-eq). This is largely due to the greater electrical energy consumption during fabrication of PZT compared to NBT. However, a closer look at Fig. 8 reveals that the materials constituents of both ceramics, the carbon footprint of Bi_2O_3 surpasses that of PbO due to the additional burden of processing and purification of bismuth and its oxide compared to PbO. If fabrication processing techniques for PZT such as the use of sintering aids becomes fully optimised thereby driving down the electrical energy consumption, the environmental profile of NBT may become worse compared to PZT. To reduce the carbon footprint of NBT, effort should therefore be geared towards improving the material processing requirements of Bi_2O_3.

In some instances such as the energy consumed in casting, extrusion, rough rolling, metal powder formation, wire-drawing, vaporization, coarse and fine machining and grinding processes, the eco-audit data for bismuth and lead are somewhat similar (typically < 5% variance) [84]. Across a range of processes for converting lead into a metal powder, larger amount of energy is consumed for the equivalent process for bismuth. On the other hand, vaporisation processes are consistently more energy intensive and consequently higher carbon footprint for bismuth than lead [84]. This explains why a tremendous amount of energy and by extension high carbon footprint is invested during the production of bismuth and its oxides. For this reason, evaporation of bismuth during sintering may pose more significant problem than the evaporation of lead, resulting in reliability issues in piezoelectric applications [23].

The major difference between lead and bismuth can be observed based on their actual extraction from the earth crust, where the overall embodied energy of primary production of lead (between 25 and 29 MJ/kg) is less than that of bismuth (between 139 and 154 MJ/kg) [60,84]. Furthermore, on a gram per gram basis, the extraction of bismuth generates a three to four-fold increase in acidification and eutrophication potentials in comparison to lead [84]. Also, during the

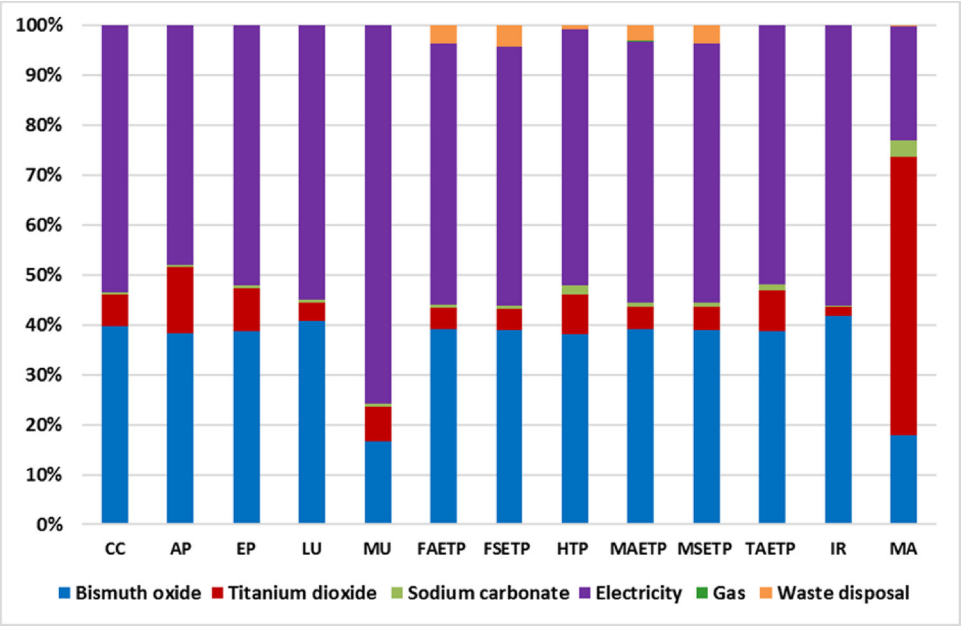

Fig. 7. Environmental profile of functional unit of 1 kg of laboratory-based NBT ceramic showing relative proportions of each of the 13 impact categories due to contributing processes. CC, Climate Change; AP, acidification potential; EP, eutrophication potential; LU, land use; MU, materials utilisation (i.e. cumulative energy demand). Five variants of ecotoxicity: fresh water aquatic, FAETP 100a; fresh water sediment, FSETP 100a; human toxicity potential, HTP 100a; marine aquatic, MAETP 100a; marine sediment, MSETP 100a; and terrestrial, TAETP 100a; are also considered alongside ionisation radiation (IR) and malodours air (MA).

extraction of bismuth, the amount of water usage is an order of magnitude greater than that for lead [60,61,84]. In terms of post-use criteria, bismuth compares unfavourably with lead due to its energetic cost of recycling, which is almost four times when compared to lead [84]. In the current supply, bismuth possesses a recycle fraction, averaging out at between 9–10% as compared to the recycling potential of lead which averages out at between 68 and 76%. The economic non-viability of recovering bismuth from increasingly small electronic components, renders it a material for one-shot applications [84].

The material with the third largest environmental impact is titanium dioxide (TiO_2), contributing 6% to climate change, 13% to acidification, 9% to eutrophication, 4% to land use and 7% to material use. It also contribute 4%, 4%, 8%, 4%, 5% and 8% respectively to fresh water aquatic ecotoxicity, fresh water sediment ecotoxicity, human toxicity, marine aquatic ecotoxicity, marine sediment ecotoxicity and terrestrial ecotoxicity impact categories. In terms of ionising radiation and malodours air, titanium dioxide contributes 2% and 56% respectively. TiO_2 is a non-hazardous mineral particle in the form of a white powder with high opacity and brilliant whiteness, hence its application in the fields of cosmetics, food, drugs, paints and inks, plastic and rubber products and many more [85,86]. Most of the environmental impact of TiO_2 emanates from production processes and waste disposal. TiO_2 pigments are produced from two prevalent methods namely, the sulphate process and the chloride process [87]. The sulphate process produces TiO_2 by

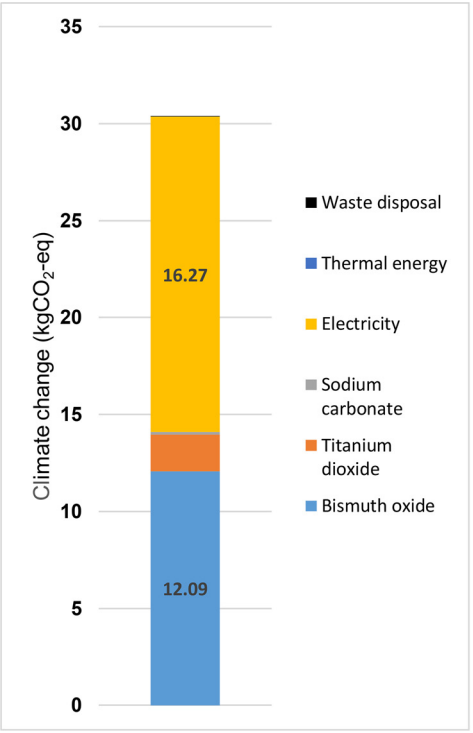

(a) Climate change impact of NBT

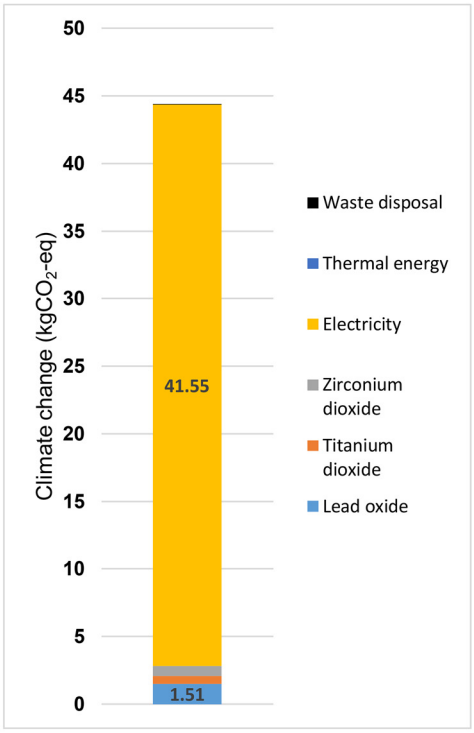

(b) Climate change impact of PZT

Fig. 8. Comparative breakdown of individual components of NBT and PZT piezoelectric ceramics under climate change impact category to highlight the most influential components. As indicated, climate change impact of bismuth oxide in NBT (Fig. 8a) outweighs that of PbO in PZT (Fig. 8b), although the overall climate change impact of PZT surpasses that of NBT due to huge difference in electrical energy consumption during fabrication. For detailed information on the data for PZT see Ibn-Mohammed et al. [25].

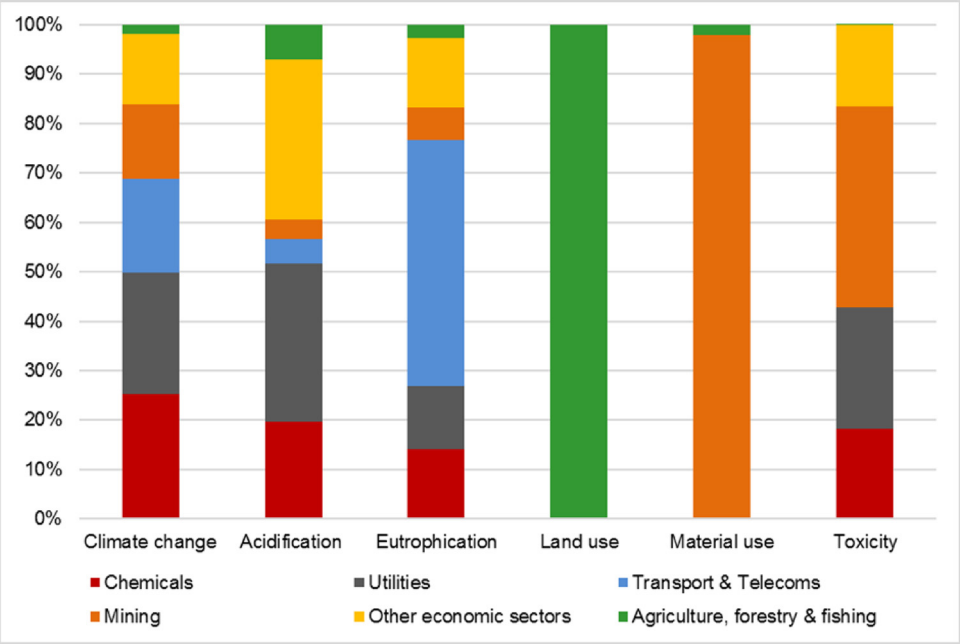

Fig. 9. IO (upstream) analysis showing the contributions of each economic sector towards the fabrication of functional unit of 1 kg of NBT ceramic in the laboratory.

treating titanium ores with concentrated sulphuric acid. The resultant titanium compound is then selectively extracted and processed into pure TiO_2. This process generates dilute sulphuric acid and large quantities of other harmful by-products, leading to the greatest amount of environmentally harmful waste per unit of TiO_2 produced. In the chloride process, natural rutile, a rare, high quality titanium ore, is treated with chlorine gas to produce titanium tetrachloride, which is then mechanically separated from the other chlorides, distilled and oxidized to produce TiO_2 [87]. Compared to the sulphate, the chloride process is 15 times cleaner but more expensive and requires high quality ores. Roughly two-third of the EU production of TiO_2 is based on the sulphate process with the remaining one-third based on the chloride process [88].

Essentially, TiO_2 itself is a useful, non-toxic and non-carcinogenic [89–94] inorganic compound, but the waste stream associated with it is extremely acidic and its methods of final disposal creates numerous environmental issues. For instance, a number of coastal production plants based on the sulphate approach dump large amount of sulphuric acid into rivers and connecting waterways. Although the alkaline sea water buffers and neutralises the dilute acidic waste, dumping sulphuric acid causes a sudden drop in pH value of the receiving water and reduces the oxygen content of the water, thereby decimating marine life. The impact on land and the high malodours air relates to the fact that sulphuric acid is also dumped into the soil and emissions released into the atmosphere. Landlocked TiO_2 production plants neutralise the acidic waste by mixing it with chalk and utilising the resultant solid to build waste dumps [87,88] but these plants release dust and gas emissions.

The environmental impact described above pertains to pigmentary TiO_2, however, research on the toxic effects of TiO_2 as a nanomaterial (ultrafine) on the ecosystem has been reported. Example include study by Shah et al. [95] on the toxicological profile of TiO_2 at the molecular level in both in vitro and in vivo systems such as living organisms or cells; Simonin et al. [85] on how TiO_2 nanoparticles (NP) strongly impact soil microbial function by affecting archaeal nitrifiers; Liu et al. [96] regarding how the interactions of TiO_2 NP with other chemicals or physical factors may result in an increase in toxicity or adverse effects and Zhu et al. [97] on the impact of TiO_2 NP on marine environment. Schilling et al. [98] reported that use of TiO_2 NP (ultrafine) in some applications, at a concentration up to 25% poses no risks to human health.

3.1.4. Input-output (upstream) emission analysis of NBT ceramics

Table 1 shows the emissions due to IO indirect (upstream) activities based on the production of NBT across five indicators. In this section, we try to analyse how these emissions are distributed across key economic sectors by considering three influential impact categories: climate change; land use and material use. This will provide relevant information regarding the key sectors to target for requisite intervention options. As shown in Fig. 9, for the case of IO GHG emissions (i.e. climate change, 6.2 $kgCO_2$-eq), the impacts are: chemical (1.6 $kgCO_2$-eq, 25.3%), utilities (1.5 $kgCO_2$-eq, 24.5%), transport & telecommunication (1.17 $kgCO_2$-eq, 19%), mining (0.93 $kgCO_2$-eq, 15.1%) and agriculture (0.12 $kgCO_2$-eq, 1.9%). All other economic sectors other than the aforementioned constitute the remaining 14.1%, 0.87 $kgCO_2$-eq. For land use (0.59 m^2a), agriculture sector is the dominant sector impacted, representing almost 100% of the entire IO upstream impact. This is based on the WIOD IO data for the agricultural sector covering arable, permanent crop, pastures and forest areas (See ESI Table S10). The two main economic sectors that contributed to the upstream material usage (42.53 MJ-eq/kg) are mining (41.69 MJ-eq/kg, 98%) and agriculture (0.84 MJ-eq/kg, 2%). As with the case of PZT vs KNN [25], of the 98% IO upstream emissions attributed to mining activities, 83% of the impact is allocated to the RoW with the remaining 17% attributed to the UK based on the MRIO framework used in this study.

3.1.5. Eco-indicator assessment of NBT ceramic fabrication

The Eco-indicator 99 results for NBT in terms of damage to the ecosystem, human health and resources are shown in Fig. 10. For definition of the three aforementioned indicators, see Ibn-Mohammed et al. [25]. As indicated, the highest impact from NBT fabrication emanates from high energy consumption, followed by bismuth oxide in that order, thereby constituting threats to human as well as aquatic species. The Eco-indicator 99 results are in agreement with the results based on CML methods described in Section 3.1.3.

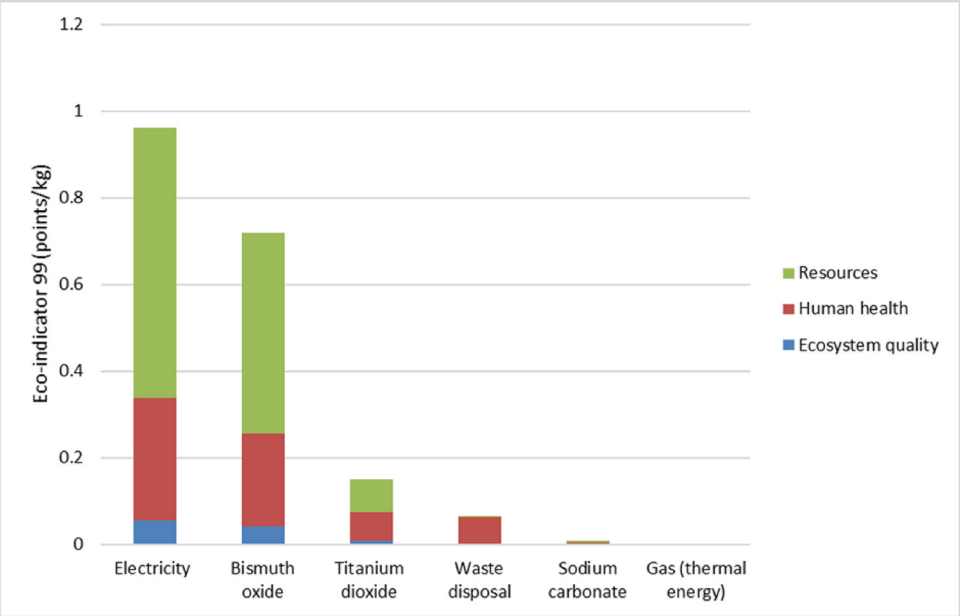

Fig. 10. Eco indicator 99 results based on functional unit of 1 kg of NBT ceramic fabricated in the laboratory.

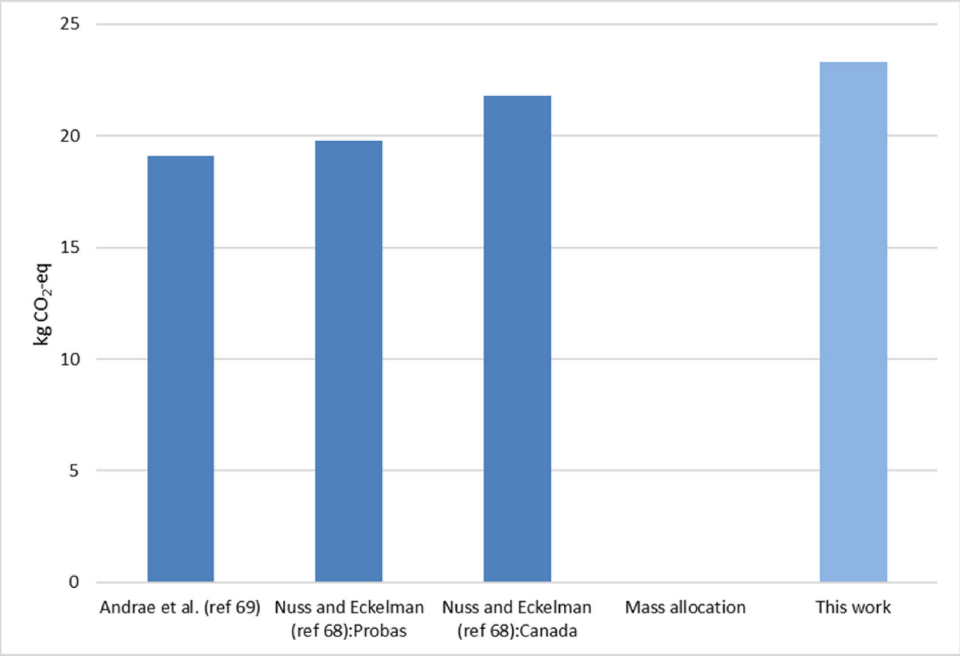

Fig. 11. Comparative emissions intensity data for bismuth based on data from literature and the data derived in this work.

3.1.6. Sensitivity analysis based on how emissions intensity of bismuth is derived

As shown in Fig. 11, the model for the determination of emissions intensity of bismuth developed by Andrae et al. [61], Nuss and Eckelman [60] (using data from both Probas and Canada) as well as in this work is based on economic allocation. Allocation by mass partitioning yields almost zero impact on bismuth since bismuth is a small fraction by mass (typically < 1%) in comparison to other co-products [59–62] thus rendering mass allocation inapplicable. Other limitations of this work especially as it pertains to economies of scale of the materials development is highlighted previously by Ibn-Mohammed et al. [25]. Further sensitivity analysis regarding the impact of location on emissions intensity of electricity consumption is provided in the ESI.

3.2. Comparison of environmental profile of NBT vs PZT vs KNN

To put the environmental profile of the NBT, PZT and KNN piezoelectric ceramics into perspective, a comparison across different indicators is provided. As shown in Fig. 12, based on the processing activities (e.g. drying, calcining and sintering) involved during fabrication, NBT consumes the lowest energy, both thermal (Fig. 12a) and electrical (Fig. 12b). As indicated in Fig. 12b, ball milling consumes a great deal of electrical energy for all three piezoelectric materials due to long duration which is 24 h (twice) for both PZT and KNN and 6 h (twice) for NBT. Irrespective of the differences in milling time of the ceramics, optimised rotational speed and the improved grinding capacity available in industry drives down the high electrical energy

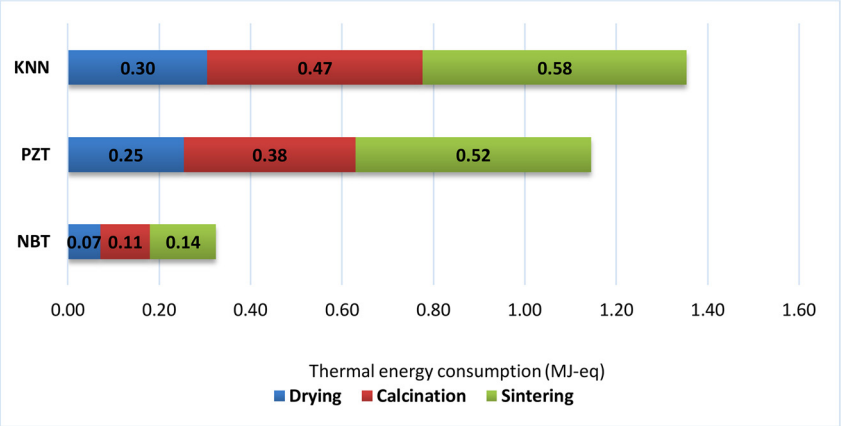

(a) Break down of thermal energy consumption across individual fabrication and processing steps. Results shown are based on a functional unit of 1 kg of piezoelectric materials produced at the laboratory scale.

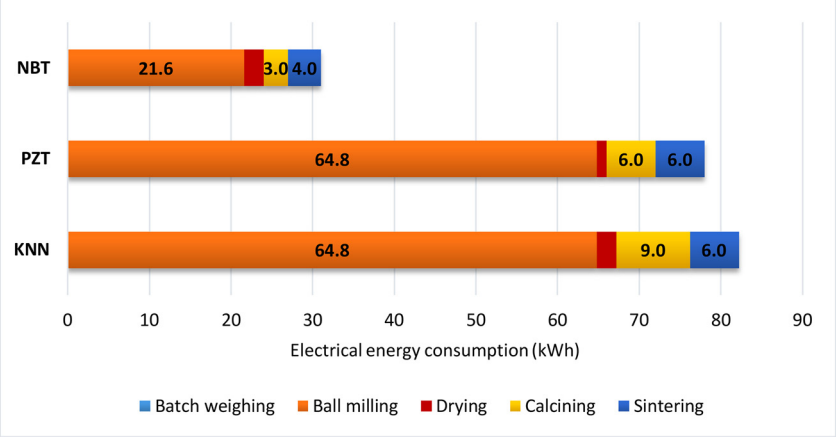

(b) Electrical energy distribution across individual fabrication and processing steps. Results shown are based on a functional unit of 1 kg of piezoelectric materials produced at the laboratory scale.

Fig. 12. Thermal (12a) and electrical (12b) energy distribution of the individual processing steps involved in the laboratory manufacturing routes of KNN, PZT and NBT. For detailed data on KNN and PZT, see Ibn-Mohammed et al. [25].

attributed to ball milling on the laboratory scale whilst maintaining control of particle size and morphology.

Fig. 13 shows the comparison of the environmental profile of the three piezoelectric ceramics across a number of environmental indicators namely: primary energy consumption and materials utilisation (Fig. 13a); toxicological impact (Fig. 13b); Eco-indicator 99 (Fig. 13c) and input-output (IO) upstream GHG emissions (Fig. 13d). As shown in Fig. 13a, NBT is responsible for the least primary energy consumption in comparison to PZT and KNN. This pertains to the fact that NBT's specific heat capacity (~101 J/kg K) [26] is notably lower than that of PZT (350 J/kg K) and KNN (420 J/kg K). This drives down NBT's primary energy demand as it consumes lower thermal energy and by extension electrical energy, during the heating cycles involved in its fabrication. As such, its environmental impact at the fabrication stage is therefore lower, although the impact of materials embedded in Bi_2O_3 (74.56 MJ-eq) within NBT is higher than that of PbO (32.07 MJ-eq) within PZT. Detailed data on the primary energy consumption attributed to the fabrication processes of both KNN and PZT is already provided in Ibn-Mohammed et al. [25] The overall comparative assessment considers five variants of toxicological impact as indicated in Fig. 13(b). As shown, the environmental toxicological profile of NBT is the lowest, although in terms of constituent materials, the toxicological impact of Bi_2O_3 outweighs that of PbO. The added toxicological impact of PZT over NBT across the entire lifecycle is attributed to high electrical energy consumption during fabrication (see Fig. 8).

Fig. 13(c) and (d) both provide further insight into the dangers to preservation and protection of ecosystem and key economic sectors by PZT, NBT and KNN. In terms of the damage to ecosystem quality, resources and human health, the production of NBT is considerably lower than that of both PZT and KNN as shown in Fig. 13(c), while Fig. 13(d) highlights detrimental effect on the upstream IO GHG for key economic sectors. Again, NBT yields lower effect on the key economic sectors highlighted compared to PZT and KNN. The lower supply chain IO GHG upstream impact of NBT is associated to its overall lower cost in terms of production and materials compared to PZT and KNN. This is particularly the case given that economic data such as cost of materials are converted into physical quantities (e.g. kg of material) in IO analysis. As such, a lower economic output produces lower upstream emissions across the supply chain of the material under consideration.

3.3. Implications of findings for piezoelectric materials researchers and policy makers

Across the years, the application of piezoelectric effect was made possible by lead-free piezoelectric materials including quartz, Rochelle salt, potassium dihydrogen phosphate and barium titanate [99]. PZT became widely used in the 1960s and deployed across different sectors resulting in a number of benefits. These include less consumption of fuel (e.g. gasoline) and cleaner air due to piezoelectric fuel-injection actuators; non-invasive medical imaging and diagnosis made possible

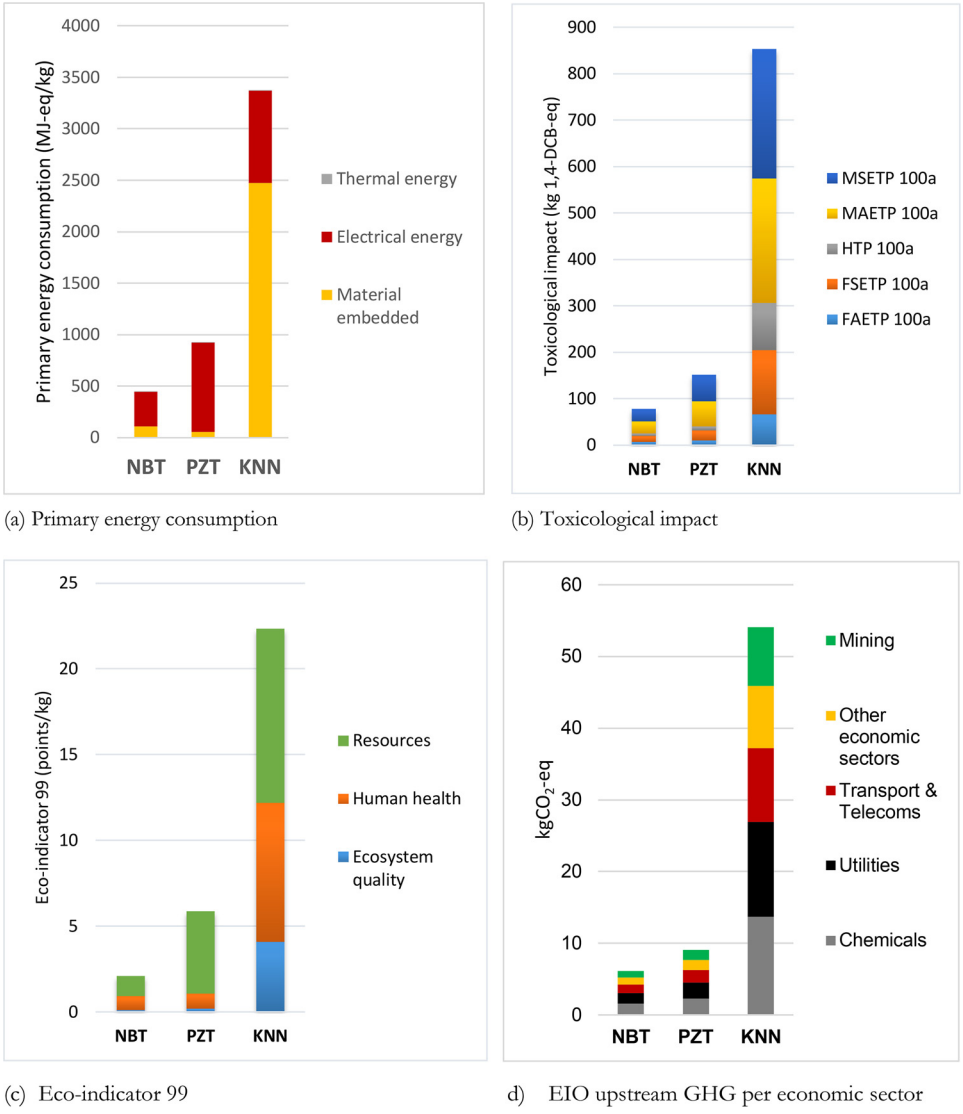

Fig. 13. Comparison of overall environmental profile of lead-based (PZT) and lead-free (KNN and NBT) piezoelectric functional ceramics. a) Primary energy demand, b) toxicological footprint, c) eco-indicator 99 comparisons, d) EIO upstream GHG comparison.

by ultrasonic piezoelectric transducers; structural health monitoring enabled by ultrasonic non-destructive testing driven by piezoelectricity and safety in transport facilitated by ultrasonic distance sensors [23]. However, despite the dominance of PZT in the piezo market, some lead-free piezoelectric materials were employed in many areas where the properties of PZT were not suitable. For instance quartz was commonly used as an oscillator in watches and filters. Also, quartz and $GaSO_4$ were used in pressure sensors – an area of application where PZT easily depolarizes at high pressures, yielding high conductivity at low frequencies and elevated temperatures, whilst exhibiting strong charge-free hysteresis [100–104]. Other areas of applications where lead-free piezo materials demonstrates competitive edge are detailed by Rödel et al. [23].

In recent times, EU legislations, prompted by the success in replacing lead in other applications (e.g. food processing equipment, lubricating greases, fishing sinkers, ceramic glazes, plumbing etc.) alongside the landmark paper by Saito et al. [5], stimulated research on the development of lead-free piezoelectric materials, leading to a sharp increase in annual publications. More than 400 refereed publications per year have since been recorded between 2010 and 2013, enabled through heavy funding from countries such as Japan [105], Korea [26], China, Germany and the UK [27].

Although criteria for exemption with RoHS recognises the consideration of lifecycle impacts of alternative materials, little thought was given to the importance of tracking the overall environmental impact of these new materials. Such importance was demonstrated by Ibn-Mohammed et al. [25] who generated debate and discussion among materials scientists regarding the overall environmental viability of lead-free materials, given the surprise finding that KNN is not intrinsically greener than PZT. Since lead-free piezoelectrics do not offer a competitive edge, it is essential that they offer a better overall environmental profile but as stated in Section 3.1.3 (Fig. 8), the overall impact of Bi_2O_3 surpasses that of PbO. The fact that 90–95% of bismuth is derived from lead smelting also diminishes the environmental edge which NBT has over PZT.

Even though KNN and NBT do not offer the expected advantages from an environmental point of view, the toxicity of PbO in PZT is still a source of major concern but there is no conclusive evidence over the actual risks associated with lead leaching into the environment from landfilling and final disposal of lead-based piezoelectric materials. In fact, there is no evidence to suggest that lead-based piezoelectrics constitute a hazard to human health during their use phase. The work previously reported by Ibn-Mohammed et al. [25] and the current paper demonstrate that lead-free piezo materials offer as great or greater an

impact with respect to PZT. In addition to environmental considerations, there are issues pertaining to reliability and processing windows as well as cost when comparing lead-free and lead-based piezo materials. For instance, evaporation of alkali metals and/or bismuth during sintering may constitute significant problem compared to the evaporation of lead. As such, the processing windows, especially with respect to lead-free piezo materials such as KNN have been reported to be very narrow and may result in reliability issues [22]. Scaling production to the required level desired for industrial applications may therefore become difficult. Niobium, a major constituent material in KNN is considerably more expensive than the raw materials for PZT. Such high cost of materials may not appeal to potential manufacturers and by extension customers. An advantage for KNN may rest in the viability of using low-cost nickel as an electrode material, which is not possible for PZT [106]. For PZT multilayer actuators, only copper and noble metal electrodes are available [23].

Several important questions therefore come to mind: i) what should lead-free piezo researchers do considering the great deal of research efforts and heavy funding and investment already put in? ii) How will findings from an LCA perspective shape the decision-making mechanism of policy makers and regulators? iii) How will the outcomes of research efforts and policy initiatives be received by the society (i.e. end users) given the strategic importance of piezoelectric materials in different human endeavours? iv) What is the overall future of lead-free piezoelectric research?

These issues must be addressed systematically on a case by case basis. The exemption enjoyed by PZT-based piezoelectrics should not be lifted especially in applications where their merit far outweighs their demerits. For example, the advantages derived from using PZT in ultrasonic medical imaging treatment and diagnosis far outweighs the health hazards from unlikely uncontrolled disposal of medical device in the environment at the end of life [23]. Accordingly, provided adequate alternatives are not available, replacement of lead-based piezoelectric materials used in critical applications should not be forced.

There is an argument that only the complete lift of the exemption on PZT will encourage further research efforts on lead-free materials but given the overall findings in this work, it will be very difficult to make a case for complete ban of lead-containing piezoelectrics. Moreover, there exist reliability issues and uncertainty about the time frame for lead-free piezoelectrics to transition from laboratory to application level (i.e. market), although such transitions are speculated upon by Rödel et al [23]. The conclusion must therefore be that the context in which a piezoelectric material is used must constitute a major consideration when its potential risks and challenges are reviewed.

4. Summary and concluding remarks

The results presented in this study indicate that, compared to both PZT and KNN, NBT does offer a better environmental profile across multiple environmental indicators due mainly to the lower energy (thermal and electrical) consumed during fabrication. However, a close comparison of NBT with PZT found that the environmental profile of Bi_2O_3 surpasses that of PbO across many indicators, including climate change. This is largely due to the additional processing and refining steps involved in bismuth production, which poses an extra challenge in metallurgical recovery. Furthermore, in terms of recyclability, bismuth compares unfavourably with lead due to its non-viable and energetic cost of recycling, rendering it a material for one-shot applications whilst threatening the upscaling potential of NBT for future piezoelectric applications. More importantly, the reliance of bismuth (roughly 90–95% of bismuth is derived as a by-product of lead) on the refining and smelting process of lead is a major source of concern.

Generally speaking, “lead-free piezoelectric materials” is a generic term that encompasses two general groups [23] (i) Piezoelectrics that compete for the same applications as PZT and (ii) those whose properties are inferior to PZT but whose ease of processing outweighs performance criteria. In competition with PZT are KNN, NBT, and to a lesser degree (Ba, Ca) $(Zr,Ti)O_3$(BCZT) based materials and they are the focus of this research. Less performant but highly integratable materials include SiO_2, AlN, ZnO, polyvinylidene fluoride (PVDF) and poly-L-lactic acid (PLLA). These latter materials have a low piezoelectric activity, no impact on the PZT market and are outside the scope of this study.

The methodological framework adopted in this research should be useful for the LCA and environmental profile assessment of other emerging materials systems and architectures at their early stages before key design, policy and operational decisions are made. It emphasises the need for materials scientists, engineers and industry to consider the entire supply chain life cycle impact of materials in design and manufacture, before deciding on the preferred substituted choice. It provides an evidence-based decision-making framework for legislative bodies, standards setting organisations and policy makers to aid their roles as enforcer of environmental responsibility with the view to safeguard the scarcity and criticality of materials resources and prevent unsustainable practices. The findings within this paper and previous studies are particularly pertinent at this time as RoHS exemptions have recently been reviewed and recommendations on lead piezoelectric materials were only extended for a three years.

Overall, through the current work, we have: (i) advanced a conversation around the need to be pragmatic, systematic and holistic in the realm of decision making for material replacement in functional applications; and (ii) demonstrated the opportunity that can be afforded by LCA and supply chain modelling to capture previously unidentified environmental hotspots in complex production and consumption systems, thereby igniting new innovation and intervention options.

Conflict of interest

There are no conflict of interest to declare.

Acknowledgments

This work was financially supported by the Engineering and Physical Sciences Research Council (EPSRC-EP/L017563/1), United Kingdom, through the University of Sheffield, under the project titled: Substitution and Sustainability in Functional Materials and Devices.

Appendix A. Supplementary data

Supplementary material related to this article can be found, in the online version, at doi:https://doi.org/10.1016/j.jeurceramsoc.2018.06.044.

References

[1] F. Cucchiella, I. D’Adamo, S.L. Koh, P. Rosa, Recycling of WEEEs: an economic assessment of present and future e-waste streams, Renew. Sustain. Energy Rev. 51 (2015) 263–272.
[2] T. Lusiola, F. Bortolani, Q. Zhang, R. Dorey, Molten hydroxide synthesis as an alternative to molten salt synthesis for producing K0.5Na0.5NbO3 lead free ceramics, J. Mater. Sci. 47 (2012) 1938–1942.
[3] J. Koruza, B. Rožič, G. Cordoyiannis, B. Malič, Z. Kutnjak, Large electrocaloric effect in lead-free K0.5Na0.5NbO3-SrTiO3 ceramics, Appl. Phys. Lett. 106 (2015) 202905.
[4] H. Zhang, C. Chen, X. Zhao, H. Deng, B. Ren, X. Li, et al., Structure and electrical properties of Na1/2 Bi1/2 TiO3–xK1/2 Bi1/2 TiO3 lead-free ferroelectric single crystals, Solid State Commun. 201 (2015) 125–129.
[5] Y. Saito, H. Takao, T. Tani, T. Nonoyama, K. Takatori, T. Homma, et al., Lead-free piezoceramics, Nature 432 (2004) 84–87.
[6] A. Nourmohammadi, M. Bahrevar, S. Schulze, M. Hietschold, Electrodeposition of lead zirconate titanate nanotubes, J. Mater. Sci. 43 (2008) 4753–4759.
[7] C. He, X. Li, Z. Wang, Y. Liu, D. Shen, T. Li, et al., Growth of Pb (Fe1/2 Nb1/2) O3–Pb (Yb1/2 Nb1/2) O3–PbTiO3 piezo-/ferroelectric crystals for high power and high temperature applications, CrystEngComm 14 (2012) 4407–4413.
[8] S. Koh, T. Ibn-Mohammed, A. Acquaye, K. Feng, I. Reaney, K. Hubacek, et al., Drivers of US toxicological footprints trajectory 1998–2013, Sci. Rep. 6 (2016) 39514.

[9] K. Reichmann, A. Feteira, M. Li, Bismuth sodium titanate based materials for piezoelectric actuators, Materials 8 (2015) 8467–8495.
[10] T. Ibn-Mohammed, S. Koh, I. Reaney, D. Sinclair, K. Mustapha, A. Acquaye, et al., Are lead-free piezoelectrics more environmentally friendly? MRS Commun. (2017) 1–7.
[11] E. Cross, Materials science: lead-free at last, Nature 432 (2004) 24–25.
[12] J. Curie, P. Curie, Développement, par pression, de l'électricité polaire dans les cristaux hémièdres à faces inclinées, Comptes Rendus 91 (1880) 294–295.
[13] R. Jaeger, L. Egerton, Hot pressing of potassium-sodium niobates, J. Am. Ceram. Soc. 45 (1962) 209–213.
[14] W. Heywang, K. Lubitz, W. Wersing, Piezoelectricity: Evolution and Future of a Technology, Springer Science & Business Media, 2008.
[15] W. Jo, R. Dittmer, M. Acosta, J. Zang, C. Groh, E. Sapper, et al., Giant electric-field-induced strains in lead-free ceramics for actuator applications – status and perspective, J. Electroceram. 29 (2012) 71–93.
[16] J. Rödel, W. Jo, K.T. Seifert, E.M. Anton, T. Granzow, D. Damjanovic, Perspective on the development of lead-free piezoceramics, J. Am. Ceram. Soc. 92 (2009) 1153–1177.
[17] H. Ledbetter, H. Ogi, N. Nakamura, Elastic, anelastic, piezoelectric coefficients of monocrystal lithium niobate, Mech. Mater. 36 (2004) 941–947.
[18] T. Karaki, M. Adachi, K. Yan, High-performance lead-free barium titanate piezoelectric ceramics, Adv. Sci. Technol. Trans. Tech. Publ. (2009) 7–12.
[19] H. Takahashi, Y. Numamoto, J. Tani, K. Matsuta, J. Qiu, S. Tsurekawa, Lead-free barium titanate ceramics with large piezoelectric constant fabricated by microwave sintering, Jpn. J. Appl. Phys. 45 (2006) L30.
[20] Kakimoto K-I, T. Yoshifuji, H. Ohsato, Densification of tungsten-bronze KBa2 Nb5 O15 lead-free piezoceramics, J. Eur. Ceram. Soc. 27 (2007) 4111–4114.
[21] P. Panda, Review: environmental friendly lead-free piezoelectric materials, J. Mater. Sci. 44 (2009) 5049–5062.
[22] J.F. Li, K. Wang, F.Y. Zhu, L.Q. Cheng, F.Z. Yao, (K, Na) NbO3-based lead-free piezoceramics: fundamental aspects, processing technologies, and remaining challenges, J. Am. Ceram. Soc. 96 (2013) 3677–3696.
[23] J. Rödel, K.G. Webber, R. Dittmer, W. Jo, M. Kimura, D. Damjanovic, Transferring lead-free piezoelectric ceramics into application, J. Eur. Ceramic Soc. 35 (2015) 1659–1681.
[24] J.-F. Li, K. Wang, F.-Y. Zhu, L.-Q. Cheng, F.-Z. Yao, (K, Na)NbO3-based lead-free piezoceramics: fundamental aspects, processing technologies, and remaining challenges, J. Am. Ceram. Soc. 96 (2013) 3677–3696.
[25] T. Ibn-Mohammed, S. Koh, I. Reaney, A. Acquaye, D. Wang, S. Taylor, et al., Integrated hybrid life cycle assessment and supply chain environmental profile evaluations of lead-based (lead zirconate titanate) versus lead-free (potassium sodium niobate) piezoelectric ceramics, Energy Environ. Sci. 9 (2016) 3495–3520.
[26] M.M. Lencka, M. Oledzka, R.E. Riman, Hydrothermal synthesis of sodium and potassium bismuth titanates, Chem. Mater. 12 (2000) 1323–1330.
[27] E. Aksel, J.L. Jones, Advances in lead-free piezoelectric materials for sensors and actuators, Sensors 10 (2010) 1935–1954.
[28] C.-S. Chou, C.-Y. Wu, R.-Y. Yang, C.-Y. Ho, Preparation and characterization of the bismuth sodium titanate (Na0.5 Bi0.5 TiO3) ceramic doped with ZnO, Adv. Powder Technol. 23 (2012) 358–365.
[29] A. Ioachim, M. Toacsan, M. Banciu, L. Nedelcu, H. Alexandru, C. Berbecaru, et al., BNT ceramics synthesis and characterization, Mater. Sci. Eng. B 109 (2004) 183–187.
[30] Y. Lin, S. Zhao, N. Cai, J. Wu, X. Zhou, C.W. Nan, Effects of doping Eu2O3 on the phase transformation and piezoelectric properties of Na0.5 Bi0.5 TiO3-based ceramics, Mater. Sci. Eng. B 99 (2003) 449–452.
[31] H. Nagata, T. Takenaka, Additive effects on electrical properties of (Bi1/2 Na1/2) TiO3 ferroelectric ceramics, J. Eur. Ceramic Soc. 21 (2001) 1299–1302.
[32] A. Watcharapasorn, S. Jiansirisomboon, T. Tunkasiri, Sintering of Fe-doped Bi0.5 Na0.5 TiO3 at < 1000 C, Mater. Lett. 61 (2007) 2986–2989.
[33] A. Watcharapasorn, S. Jiansirisomboon, Grain growth kinetics in Dy-doped Bi0.5 Na0.5 TiO3 ceramics, Ceram. Int. 34 (2008) 769–772.
[34] C.-S. Chou, J.-H. Chen, R.-Y. Yang, S.-W. Chou, The effects of MgO doping and sintering temperature on the microstructure of the lead-free piezoelectric ceramic of Bi0.5 Na0.5 TiO3, Powder Technol. 202 (2010) 39–45.
[35] C.-S. Chou, R.-Y. Yang, J.-H. Chen, S.-W. Chou, The optimum conditions for preparing the lead-free piezoelectric ceramic of Bi0.5 Na0.5 TiO3 using the taguchi method, Powder Technol. 199 (2010) 264–271.
[36] T. Ibn-Mohammed, R. Greenough, S. Taylor, L. Ozawa-Meida, A. Acquaye, Operational vs. embodied emissions in buildings—a review of current trends, Energy Build. 66 (2013) 232–245.
[37] A. Acquaye, K. Feng, E. Oppon, S. Salhi, T. Ibn-Mohammed, A. Genovese, et al., Measuring the environmental sustainability performance of global supply chains: a multi-regional input-output analysis for carbon, sulphur oxide and water footprints, J. Environ. Manage. 187 (2017) 571–585.
[38] A.A. Acquaye, T. Wiedmann, K. Feng, R.H. Crawford, J. Barrett, J. Kuylenstierna, et al., Identification of 'carbon hot-spots' and quantification of GHG intensities in the biodiesel supply chain using hybrid LCA and structural path analysis, Environ. Sci. Technol. 45 (2011) 2471–2478.
[39] D. Collado-Ruiz, H. Ostad-Ahmad-Ghorabi, Comparing LCA results out of competing products: developing reference ranges from a product family approach, J. Clean. Prod. 18 (2010) 355–364.
[40] A.Y. Hoekstra, T.O. Wiedmann, Humanity's unsustainable environmental footprint, Science 344 (2014) 1114–1117.
[41] A. Azapagic, C. Pettit, P. Sinclair, A life cycle methodology for mapping the flows of pollutants in the urban environment, Clean Technol. Environ. Policy 9 (2007) 199–214.
[42] Y. Zhang, B.R. Bakshi, E.S. Demessie, Life cycle assessment of an ionic liquid versus molecular solvents and their applications, Environ. Sci. Technol. 42 (2008) 1724–1730.
[43] L. Smith, T. Ibn-Mohammed, S.L. Koh, I.M. Reaney, Life cycle assessment and environmental profile evaluations of high volumetric efficiency capacitors, Appl. Energy 220 (2018) 496–513.
[44] Ecoinvent. Ecoinvent database. 2017.
[45] S.L. Koh, A. Genovese, A.A. Acquaye, P. Barratt, N. Rana, J. Kuylenstierna, et al., Decarbonising product supply chains: design and development of an integrated evidence-based decision support system–the supply chain environmental analysis tool (SCEnAT), Int. J. Prod. Res. 51 (2013) 2092–2109.
[46] T. Ibn-Mohammed, R. Greenough, S. Taylor, L. Ozawa-Meida, A. Acquaye, Integrating economic considerations with operational and embodied emissions into a decision support system for the optimal ranking of building retrofit options, Build. Environ. 72 (2014) 82–101.
[47] S. Suh, M. Lenzen, G.J. Treloar, H. Hondo, A. Horvath, G. Huppes, et al., System boundary selection in life-cycle inventories using hybrid approaches, Environ. Sci. Technol. 38 (2004) 657–664.
[48] T. Ibn-Mohammed, S.C.L. Koh, I.M. Reaney, A. Acquaye, G. Schileo, K. Mustapha, et al., Perovskite solar cells: an integrated hybrid lifecycle assessment and review in comparison with other photovoltaic technologies, Renew. Sustain. Energy Rev. 80 (2017) 1321–1344.
[49] A. Ahmed, I. Hassan, T. Ibn-Mohammed, H. Mostafa, I.M. Reaney, L.S. Koh, et al., Environmental life cycle assessment and techno-economic analysis of triboelectric nanogenerators, Energy Environ. Sci. 10 (2017) 653–671.
[50] A.A. Acquaye, A.P. Duffy, Input–output analysis of Irish construction sector greenhouse gas emissions, Build. Environ. 45 (2010) 784–791.
[51] T. Ibn-Mohammed, Retrofitting the Built Environment: An Economic and Environmental Analysis of Energy Systems, Cambridge Scholars Publishing, 2017.
[52] T. Wiedmann, R. Wood, J.C. Minx, M. Lenzen, D. Guan, R. Harris, A carbon footprint time series of the UK–results from a multi-region input–output model, Econ. Syst. Res. 22 (2010) 19–42.
[53] ISO I. 14040: Environmental management–life cycle assessment–principles and framework. London: British Standards Institution. 2006.
[54] ISO I. TS 14067: 2013: Greenhouse Gases—Carbon Footprint of Products—Requirements and Guidelines for Quantification and Communication. International Organization for Standardization, Geneva, Switzerland. 2013.
[55] G. Geisler, T. Hofstetter, K. Hungerbühler, Production of fine and speciality chemicals: procedure for the estimation of LCIs, Int. J. LCA 9 (2004) 101–113.
[56] Angino EE, Long DT. Geochemistry of bismuth: Dowden Hutchinson and Ross; 1979.
[57] A. Naumov, World market of bismuth: a review, Russ. J. Non-Ferrous Metals 48 (2007) 10–16.
[58] Terrado AN. The bismuth metal: the metallurgy of bismuth. 2013.
[59] D. Howell, B. Dohnt, The accurate determination of bismuth in lead concentrates and other non-ferrous materials by AAS after separation and preconcentration of the bismuth with mercaptoacetic acid, Talanta 29 (1982) 391–395.
[60] P. Nuss, M.J. Eckelman, Life cycle assessment of metals: a scientific synthesis, PLoS One 9 (2014) e101298.
[61] A.S. Andrae, N. Itsubo, H. Yamaguchi, A. Inaba, Life cycle assessment of Japanese high-temperature conductive adhesives, Environ. Sci. Technol. 42 (2008) 3084–3089.
[62] A.K. Das, R. Chakraborty, M.L. Cervera, M. de la Guardia, Analytical techniques for the determination of bismuth in solid environmental samples, TrAC Trends Anal. Chem. 25 (2006) 599–608.
[63] J.B. Guinée, R. Heijungs, G. Huppes, Economic allocation: examples and derived decision tree, Int. J. LCA 9 (2004) 23–33.
[64] F. Ardente, M. Cellura, Economic allocation in life cycle assessment, J. Ind. Ecol. 16 (2012) 387–398.
[65] A. Zamagni, J. Guinée, R. Heijungs, P. Masoni, A. Raggi, Lights and shadows in consequential LCA, Int. J. LCA 17 (2012) 904–918.
[66] W.W. Leontief, Input-Output Economics, Oxford University Press on Demand, 1986.
[67] R.E. Miller, P.D. Blair, Input-Output Analysis: Foundations and Extensions, Cambridge University Press, 2009.
[68] J. Barrett, K. Scott, Link between climate change mitigation and resource efficiency: a UK case study, Glob. Environ. Change 22 (2012) 299–307.
[69] J. Kitzes, An introduction to environmentally-extended input-output analysis, Resources 2 (2013) 489–503.
[70] T. Ten Raa, The extraction of technical coefficients from input and output data, Econ. Syst. Res. 19 (2007) 453–459.
[71] J.C. Minx, T. Wiedmann, R. Wood, G.P. Peters, M. Lenzen, A. Owen, et al., Input–output analysis and carbon footprinting: an overview of applications, Econ. Syst. Res. 21 (2009) 187–216.
[72] J.-J. Ferng, Applying input–output analysis to scenario analysis of ecological footprints, Ecol. Econ. 69 (2009) 345–354.
[73] WIOD. World Input-Output Database 2012.
[74] S. Suh, G. Huppes, Methods for life cycle inventory of a product, J. Clean. Prod. 13 (2005) 687–697.
[75] P.G. McGregor, J.K. Swales, K. Turner, The CO2 'trade balance'between Scotland and the rest of the UK: performing a multi-region environmental input–output analysis with limited data, Ecol. Econ. 66 (2008) 662–673.
[76] K. Turner, M. Lenzen, T. Wiedmann, J. Barrett, Examining the global environmental impact of regional consumption activities—part 1: a technical note on combining input–output and ecological footprint analysis, Ecol. Econ. 62 (2007) 37–44.

[77] A.A. Acquaye, F.A. Yamoah, K. Feng, An integrated environmental and fairtrade labelling scheme for product supply chains, Int. J. Prod. Econ. 164 (2015) 472–483.
[78] G.P. Peters, E.G. Hertwich, The application of multi-regional input-output analysis to industrial ecology, Handbook of Input-Output Economics in Industrial Ecology, Springer, 2009 p. 847–863.
[79] M. Lenzen, D. Moran, K. Kanemoto, A. Geschke, Building Eora: a global multi-region input–output database at high country and sector resolution, Econ. Syst. Res. 25 (2013) 20–49.
[80] J. Guo, S.S. Berbano, H. Guo, A.L. Baker, M.T. Lanagan, C.A. Randall, Cold sintering process of composites: bridging the processing temperature gap of ceramic and polymer materials, Adv. Funct. Mater. 26 (2016) 7115–7121.
[81] J. Guo, H. Guo, A.L. Baker, M.T. Lanagan, E.R. Kupp, G.L. Messing, et al., Cold sintering: a paradigm shift for processing and integration of ceramics, Angew. Chem. 128 (2016) 11629–11633.
[82] A. Baker, H. Guo, J. Guo, C. Randall, Utilizing the cold sintering process for flexible–printable electroceramic device fabrication, J. Am. Ceram. Soc. 99 (2016) 3202–3204.
[83] Ku A., Shapiro A., Kua A., Ogunseitan O., Saphores J., Schoenung J. Lead-free solders: issues of toxicity, availability and impacts of extraction 2003.
[84] P. Ion, Bismuth-a potential life-saver, Res. World Mag. (2012) 34–36 [Accessed 10th March, 2018] https://s1.q4cdn.com/337451660/files/120701%20-%20Resource%20World%20%E2%80%93%20Bismuth%20a%20potential%20life-saver.pdf.
[85] M. Simonin, A. Richaume, J.P. Guyonnet, A. Dubost, J.M. Martins, T. Pommier, Titanium dioxide nanoparticles strongly impact soil microbial function by affecting archaeal nitrifiers, Sci. Rep. 6 (2016).
[86] D.M. Brunette, P. Tengvall, M. Textor, P. Thomsen, Titanium in Medicine: Material Science, Surface Science, Engineering, Biological Responses and Medical Applications, Springer Science & Business Media, 2012.
[87] M.J. Gázquez, J.P. Bolívar, R. Garcia-Tenorio, F. Vaca, A review of the production cycle of titanium dioxide pigment, Mater. Sci. Appl. 2014 (2014).
[88] European Commission. Waste - Titanium Dioxide. 2016.
[89] P. Boffetta, V. Gaborieau, L. Nadon, M.-E. Parent, E. Weiderpass, J. Siemiatycki, Exposure to titanium dioxide and risk of lung cancer in a population-based study from montreal, Scand. J. Work Environ. Health (2001) 227–232.
[90] P. Boffetta, A. Soutar, J.W. Cherrie, F. Granath, A. Andersen, A. Anttila, et al., Mortality among workers employed in the titanium dioxide production industry in Europe, Cancer Causes Control 15 (2004) 697–706.
[91] J.L. Chen, W.E. Fayerweather, Epidemiologic study of workers exposed to titanium dioxide, J. Occup. Environ. Med. 30 (1988) 937–942.
[92] J.P. Fryzek, B. Chadda, D. Marano, K. White, S. Schweitzer, J.K. McLaughlin, et al., A cohort mortality study among titanium dioxide manufacturing workers in the United States, J. Occup. Environ. Med. 45 (2003) 400–409.
[93] D.H. Garabrant, L.J. Fine, C. Oliver, L. Bernstein, J.M. Peters, Abnormalities of pulmonary function and pleural disease among titanium metal production workers, Scand. J. Work Environ. Health (1987) 47–51.
[94] A.V. Ramanakumar, M.É Parent, B. Latreille, J. Siemiatycki, Risk of lung cancer following exposure to carbon black, titanium dioxide and talc: results from two case–control studies in Montreal, Int. J. Cancer 122 (2008) 183–189.
[95] S.N.A. Shah, Z. Shah, M. Hussain, M. Khan, Hazardous effects of titanium dioxide nanoparticles in ecosystem, Bioinorg. Chem. Appl. 2017 (2017).
[96] K. Liu, X. Lin, J. Zhao, Toxic effects of the interaction of titanium dioxide nanoparticles with chemicals or physical factors, Int. J. Nanomed. 8 (2013) 2509–2520.
[97] X. Zhu, J. Zhou, Z. Cai, TiO2 nanoparticles in the marine environment: impact on the toxicity of tributyltin to abalone (Haliotis diversicolor supertexta) embryos, Environ. Sci. Technol. 45 (2011) 3753–3758.
[98] K. Schilling, B. Bradford, D. Castelli, E. Dufour, J.F. Nash, W. Pape, et al., Human safety review of “nano” titanium dioxide and zinc oxide, Photochem. Photobiol. Sci. 9 (2010) 495–509.
[99] Cady W. Piezoelectricity, Vol. II. Dover Publications, New York; 1964.
[100] D. Berlincourt, H. Krueger, B. Jaffe, Stability of phases in modified lead zirconate with variation in pressure, electric field, temperature and composition, J. Phys. Chem. Solids 25 (1964) 659–674.
[101] H. Krueger, D. Berlincourt, Effects of high static stress on the piezoelectric properties of transducer materials, J. Acoust. Soc. Am. 33 (1961) 1339–1344.
[102] M. Morozov, D. Damjanovic, Charge migration in Pb (Zr, Ti) O3 ceramics and its relation to ageing, hardening, and softening, J. Appl. Phys. 107 (2010) 034106.
[103] Q. Zhang, W. Pan, S. Jang, L. Cross, Domain wall excitations and their contributions to the weak-signal response of doped lead zirconate titanate ceramics, J. Appl. Phys. 64 (1988) 6445–6451.
[104] H.H. Krueger, Stress sensitivity of piezoelectric ceramics: part 1. Sensitivity to compressive stress parallel to the polar axis, J. Acoust. Soc. Am. 42 (1967) 636–645.
[105] H. Yabuta, M. Shimada, T. Watanabe, J. Hayashi, M. Kubota, K. Miura, et al., Microstructure of BaTiO3–Bi (Mg1/2Ti1/2) O3–BiFeO3 piezoelectric ceramics, Jpn. J. Appl. Phys. 51 (2012) 09LD4.
[106] S. Kawada, M. Kimura, Y. Higuchi, H. Takagi, (K, Na) NbO3-based multilayer piezoelectric ceramics with nickel inner electrodes, Appl. Phys. Express 2 (2009) 111401.